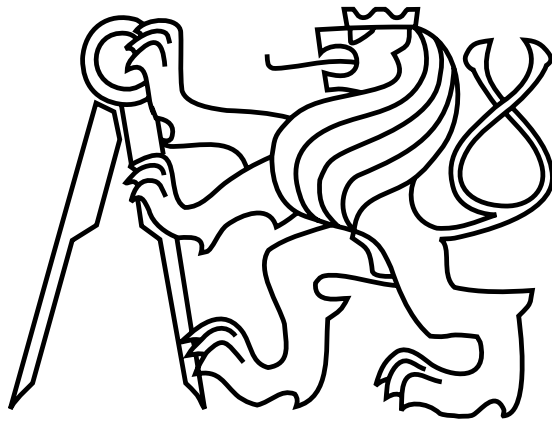


CZECH TECHNICAL UNIVERSITY IN
PRAGUE

Faculty of Civil Engineering

Department of Concrete and Masonry Structures



Diploma Thesis

Prague, June 2016

Nadezda Albert



ZADÁNÍ DIPLOMOVÉ PRÁCE

I. OSOBNÍ A STUDIJNÍ ÚDAJE

Příjmení: Albert Jméno: Nadezda Osobní číslo: 371947

Zadávající katedra: K133

Studijní program: (N3607) Stavební inženýrství

Studijní obor: (3608T008) Konstrukce pozemních staveb

II. ÚDAJE K DIPLOMOVÉ PRÁCI

Název diplomové práce: Evaluation and Applicability of Visual Concrete Surface

Název diplomové práce anglicky: Evaluation and Applicability of Visual Concrete Surface

Pokyny pro vypracování:

In the study case compare treated and untreated samples for their capability of water penetration reduction, withstanding chemical damage, maintaining its visual characteristics.

Evaluate the effectiveness of the treatment.

Discuss durability and applicability of studied surfaces.

Seznam doporučené literatury:

Jméno vedoucího diplomové práce: doc. Ing. Petr Štemberk, Ph.D

Datum zadání diplomové práce: 4.3.2016

Termín odevzdání diplomové práce: 22.5.2016

Podpis vedoucího práce

Podpis vedoucího/katedry

III. PŘEVZETÍ ZADÁNÍ

Beru na vědomí, že jsem povinen vypracovat diplomovou práci samostatně, bez cizí pomoci, s výjimkou poskytnutých konzultací. Seznam použité literatury, jiných pramenů a jmen konzultantů je nutné uvést v diplomové práci a při citování postupovat v souladu s metodickou příručkou ČVUT „Jak psát vysokoškolské závěrečné práce“ a metodickým pokynem ČVUT „O dodržování etických principů při přípravě vysokoškolských závěrečných prací“.

5.3.2016

Datum převzetí zadání

Podpis studenta(ky)

DECLARATION

I, Nadezda Albert, confirm that this diploma thesis submitted for assessment was worked out only by me, under the guidance of my supervisor Assoc.Prof. Petr Štemberk, Ph.D. Any uses made within it of the works of other authors in any form (e.g. ideas, equations, figures, text, tables, programmes) are properly acknowledged at the point of their use. A full list of the references employed has been included.

Signed:

Date:

ACKNOWLEDGEMENTS

Special thanks should be given to Assoc.Prof. Petr Štemberk, Ph.D, my master thesis supervisor for his valuable support and professional guidance and to CTU Experimental Center and Ing. Pavel Reiterman, Ph.D. I wish to thank Miloš Sedláček for his assistance in photo studio. I would also like to acknowledge Bc. Jiří Němeček for his input in abrasive testing and Ing. Martin Petřík, Ph.D for his advices regarding image processing in MATLAB. I extend my deep appreciation to Michal Gabor for his attention and invaluable help during preparation of the samples, and also to his colleague Jaroslav Chramosta for interest and optimism. I wish to thank Bc. Jakub Rozumek, for his guidance through the LaTeX coding and helped with the final formatting of this document. Finally, I earnestly thank my family for their support, patience and encouragement throughout the preparation of this work.

Evaluation and Applicability of Visual Concrete Surface

ABSTRACT

This work presents experimental data used for evaluation of the effectiveness of decorative concrete finishes for proposed high strength mortar (HSM). The effect of different surface treatments was evaluated by absorption characteristics of the surface and comparison of abrasive damage results. Matlab Image Processing toolbox was used to evaluate capabilities of studied surfaces to maintain visual characteristics after food and household chemicals damage. The transition of the brightness intensity of the cured HSM throughout time was illustrated. The test results demonstrate that the mechanical treatment enhances the efficiency of the impregnation product both in terms of water penetration reduction and resistance to abrasive wear. Overall the apparent improve the performance of studied finishes can be distinguished only for the short action of a chemical agent and for the limited duration of contact with the water because none of the treatment methods creates a barrier protection on the surface.

Keywords: *Decorative concrete, image processing, near-surface properties, concrete finishes, concrete color, high-strength mortar*

Contents

1	INTRODUCTION	4
2	STATE OF THE ART	6
2.1	Near-surface concrete protection Preparation of the surface	6
2.2	Durability	7
2.2.1	Microstructure and moisture movement	7
2.2.2	Acidic damage	8
2.3	Visual assessment of concrete	10
2.3.1	Obtaining of an Image	11
2.3.2	Discoloration during early age	11
2.3.3	Effect of the curing on stability of color	13
3	OBJECTIVES	19
4	EXPERIMENTAL INVESTIGATION	20
4.1	Mix design and preparation	20
4.1.1	Mixture proportions	20
4.1.2	Mixing procedure	24
4.1.3	Curing regime	24
4.1.4	Basic physical properties	25
4.2	Description of tested samples	26
4.3	Schedule of the experimental part	29
4.4	Water absorption test	30
4.4.1	Results interpretation	31
4.4.2	Comparison of results	34
4.5	Chemical attack test	35
4.5.1	Image processing	38
4.5.2	Results interpretation	39
4.6	Abrasive wear test	43
4.6.1	Experiment procedure	43
4.6.2	Results Interpretation	45
5	SUMMARY	46
5.1	General conclusions	46
5.2	Applicability	47
5.3	Future research recommendations	48
	Bibliography	49
	List of Figures	52
	List of Tables	54

Appendices	55
A Matlab Syntax	56
B Technical lists	63
C Matlab graphical output of image processing	69

1 INTRODUCTION



Fig. 1: Black web, pattern by Sarah Arnett. White concrete. Adopted from [1]

Decorative concrete elements have become increasingly popular in contemporary architecture and interior design. Recent developments leading to new possibilities have inspired architects and designers to innovative and exciting solutions. There are a huge number of projects appearing every year that display different faces of concrete and its flexibility of utilization. It's almost inexhaustible design and artistic potential and evolving innovations in how it's applied make concrete an exceptionally fascinating and valuable building material for architecture concepts. Special mortars or concretes can be cast in almost any form or texture. By combination of forms, textures and color, not only in shades of gray, it became possible to meet many aesthetics and practical requirements of modern architecture.

Utilization of glass or highly smooth plastics as a formwork results in “glaze” even mirror-like finish of hardened concrete. This type of surface seems to be flawless and broadens the language of decorative concrete. Is it easy to integrate that technique in practice? Surfaces commonly have a thin and relatively weak upper layer - laitance (surface hydrated cement), removal of which is favourable. At the same time obtained character of laitance brings new valuable quality for decorative surface - glossy look, the appearance that is usually associated with high-priced polishing or epoxy coverings.

Common processing of the surface assumes variations of mechanical treatment and further on sealing of surface against aggressive environment that possess material degradation and visual degradation of its face. Long-term performance of the chosen treatment is a challenging issue in application of various treatments and coverings as well as long-term performance of the base cementitious material on which the product was applied. Jayson and Helsel for the Journal of Architectural Coatings:

“A horizontal concrete surface may convey the appearance of a relatively monolithic, static form. This impression can prove highly deceptive, however, thanks to the dynamic forces exerted by moisture, surface profile, and surface chemistry.” [2]

Wilco precast is one of the companies specializing in decorative concrete finishes for architecture concrete. Their offer includes production of the wide range of visual concrete surfaces: off-form finishes, rough-sawn timber finishes, chemically retarded exposed aggregate (also known as graphic concrete), grit-blasted, acid-etched finishes, honed or polished, formliners [3]. And yet their advice is to avoid gloss finishes due to the high cost of surface preparation necessary to provide a satisfactory appearance. Possibly the original glossy surface may be feasible and can serve an alternative solution. The following question arise:

Is it possible to maintain the original texture?

Is it always necessary to remove the top surface layer?

What the surface sustain without the barrier protection?

Can the mix design provide sufficient durability, stability of colour and texture of decorative surface?

Can the minimizing treatment expenses be a cost efficient solution?

These issues gave an impulse for the closer look on evaluation of visual surfaces and motivated author to write this master thesis.

2 STATE OF THE ART

2.1 Near-surface concrete protection Preparation of the surface

Studying long-term performance of the treatments Benn [4] notes the lack of recommendations on the use of different surface preparation methods for different near-surface concrete qualities. This problem is connected to endless eventualities that affect the near-surface concrete quality such as degree of curing, curing methods and curing conditions at the time of construction. Gaul [5] accentuates that great care is usually taken in selecting and installing coatings (barrier systems), insufficient attention is given to the concrete surface to which the barrier system will be attached. Gaul also writes about need in systematic approach for identification of a surface condition requirements for a particular treatment system. Identification of proper methods to correct deficiencies in the surface before application is of great importance too because specifications as “clean, dry and sound surface” cannot adequately define preparation requirements in Gaul’s opinion.

International Concrete Repair Institute (ICRI) partly helps to solve this issue, presents a classification for concrete surface profiles based on roughness. ICRI designates the CSPs in the ICRI Guideline No. 310.2R-1997, Selecting and Specifying Concrete Surface Preparation for Sealers, Coatings, Polymer Overlays and Concrete Repair. Certain degree of roughness is a key parameter for adhesion of film-forming coatings such as for example acrylic or polyurethane sealers. ICRI also indicates which methods of surface preparation can be used to render the indicated concrete surface profile. In ascending order those are: grinding, acid etching that provides up to 0.25 mm roughness, needle scaling. Over 1mm roughness can be achieved by abrasive blasting, shotblasting, water jetting, scarifying, and retarding of freshly poured surface by chemicals. Infographics below is adopted from the Blast Journal online publisher [6].

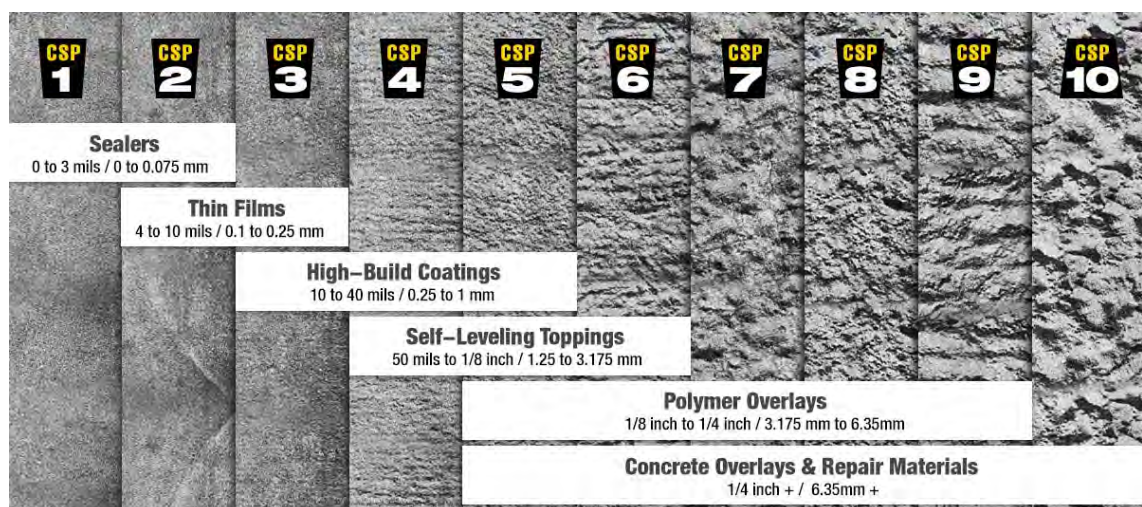


Fig. 2: 10 grades of surface of roughness for different treatment types

Without adequate surface preparation film-forming coatings are put at risk of debonding, blistering, peeling and chipping of the product.



Fig. 3: From left to right: epoxy coating failure [7], blushing and bond failure, bubbles in a sealer [8]

2.2 Durability

2.2.1 Microstructure and moisture movement

Zhang and Zong [9] presented an experimental study of the influence of water absorption on the durability of concrete materials. After 28-days curing, compressive strength, permeability, sulfate attack, and chloride ion diffusion of concrete samples were investigated. Obtained results showed that only surface water absorption related to the performance of concrete. Nevertheless surface water absorption and internal water absorption had no clear relationship for example with compressive strength; simple evaluation of concrete strength by water absorption has not been investigated. However, surface water absorption can be applied to predict in prediction of some performance characteristics of concrete, including compressive strength, permeability, resistance to sulfate attack, and chloride ion diffusion [9].

Well known fact is that supplementary cementing materials (SCMs) contribute to the hydration of Portland cement. Phenomena as pozzolanic activity and the micro-filling are associated with the use of SCMs and both contribute to enhanced mechanical characteristics and reduced permeability, thus play a key role in achieving positive long-term performance. An interesting conclusion followed the investigation by Shannag [10]. He was using a combination of natural pozzolan and silica fume to produce mortars and concretes with a compressive strength in range of 69 - 110 MPa and observed that certain combinations contribute more compressive strength, elastic modulus and workability of mixtures while other less, or also less is the contribution of silica fume or natural pozzolan when used alone. Highest strength increase gained when silica fume was used as 15% of the weight of cement replacement in the presence of 15% of natural pozzolan replacement.

In the case of metakaolin utilization by Siddique [11] all mixtures showed low water absorption. Test results indicated that with the increase in MK content from 5% to 15%, there was a decrease in the initial surface absorption, decrease in the sorptivity till 10% metakaolin replacement. But at 15% MK replacement an increase in sorptivity was observed. Analogous trend as mention earlier in this paper was observed in Siddique's investigation namely compressive strength that shares an inverse relation with sorptivity. Interesting observation includes one where MK replacements of 15% are not helpful in improving inner core durability but helps in improving surface durability characteristics.

The surface layer of concrete is the first line of defense against the ingress of aggressive agents and hence, the characteristics of this layer of concrete determine the rate of transport of the various aggressive substances into the concrete. The moisture along with chlorides and dissolved oxygen will be absorbed into the concrete cover by capillary forces depending on the degree of saturation of the concrete. Hence an assessment of the rate of ingress of chlorides has become very important for evaluating the long-term performance of concrete structures [12].

Use of dense, high-performance mortars can also inhibit biological stains. In the experimental study [13] concrete was examined as underlying material for growth of the microorganisms. Pieces of concrete stained by biological growth were observed using optical and electron microscopies. The results showed that biological stains due to algal developments, whose presence depends on the amount of moisture on the concrete wall, are in direct dependence with the porosity of the underlying material.

2.2.2 Acidic damage

The near-surface quality of the concrete are also affected by the aggressive environments where the surface is situated such as physical abrasion or chemical attack from agents such as soft water and acidic pollutants. When used in interior concrete mainly got attacked chemically which is the cause of stains or change of texture. Lifespan of visual concrete is also shortens by abrasive loading which causes scratches on concrete surface, destroying existing protective layer. Concrete furniture can be kept in intact condition with the help of epoxy sealers or throughout maintenance with penetrating sealer and wax. However penetrating sealers do not prevent stains completely. Epoxy sealers are fairly stainproof although they stretch and could be destroyed after exposure to high temperatures [14].

Concrete is susceptible to acid attack because of its alkaline nature. The components of the cement paste break down during contact with acids [15].

From the stand point of Portland cement concrete, most industrial and natural waters can be categorized as aggressive. However, the rate of chemical attack and decomposition of concrete depends on:

- the pH of the aggressive fluid

- the solubility of the acid calcium salts
- the porosity and permeability of the cement paste
- the fluid transport through the concrete.

When the permeability of concrete is low and the pH of aggressive water is above 6.5, the rate of chemical attack is considered slow. Higher pH concentration imply the chemical attack:

Property	XA1	XA2	XA3
pH	5.5 - 6.5	4.5 - 5.5	4.0 - 4.5
Severity	Weak	Medium	Strong

Tab. 1: Exposure classes for chemical attack according to DIN EN 206-1 [16]

Insoluble calcium salts may precipitate in the voids and can slow down the attack. Acids such as nitric acid, hydrochloric acid and acetic acid are very aggressive and cause high damaging effect as their calcium salts are readily soluble and removed from the attack front. Other acids such as phosphoric acid and humic acid are less harmful as their calcium salt, due to their low solubility, inhibits the attack by blocking the pathways within the concrete such as interconnected cracks, voids and porosity [15].

Roy and Arjunan [17] showed interesting trends with respect to acidic resistance. Substitution of silica fumes, metakaolin or fly ash under certain conditions has been shown to increase the chemical resistance of such mortars over those made with plain Portland cement. Chemical resistance increased in the order of silica fumes (SF) to metakaolin (MK) to fly ash (FA) series as the replacement level is increased from 0 – 10 wt.% and decreased replacement levels 15 – 30 wt.% level. But overall fly ash was evaluated to be as effective in chemical resistance as SF and MK. Interesting observation was made with regards to effect of w/c ratio: chemical resistance increased with change from 0.36 to 0.40 w/c. Compressive strength increased in the order of FA to SF to MK. No significant change in compressive strength was found as a function of replacement level for SF and MK series.

The most important properties of concrete are its strength (how much load it can support) and its durability (how long it will last in its environment). To a first approximation, these are both controlled by the cement paste rather than by the aggregate. In the case of strength, this is because the aggregate particles are normally much stronger than the cement paste, so the concrete fails when the strength of the weaker cement paste matrix is exceeded. A similar situation occurs with durability.

Cement paste is inherently more susceptible to environmental damage than the aggregate due to its pore system, which allows water and dissolved ions to enter and leave the paste. General rule is that the closer to the surface the weaker is the concrete. Degradation

of concrete happens alongside with the moisture movement from the surface through its structure. Surface durability characteristics are vital for shielding and protection of the inner material from the penetration of aggressive substances.

Measurements of the permeability of concrete can be used as an indication of durability as in [18]. Evaluation of the degree of degradation can be approached either by using visual methods or through measuring the residual mechanical properties [19].

2.3 Visual assessment of concrete

The ease of obtaining uniformity in color is directly related to the ingredients supplying the color. Whenever possible, the basic color should be established using colored fine or coarse aggregates and pigments to blend the aggregates and the matrix. Nawy [20] recommends avoiding extreme color differences between aggregate and matrix. The color should be judged from a full-size sample that is finished in accordance with planned production techniques. Changes of the texture as well as application of protective coats may transform the perception of the visual surface. Mineral admixtures may also affect color. Silica fume and fly ash depending on their carbon content will darken the hardened cement paste, while addition of limestone and cement slag result in lighter cement paste [21]. Not less important is to remember that perception of color and texture are influenced by the light source. When selecting color of concrete lighting conditions should be similar to those under which the visual concrete is intended to be viewed. Color and color tone represent relative values [20].

It is not easy to fulfill requirements for the visual concrete to be smooth, uniformly colored and free of bugholes. Casting of the samples in investigation made by Klovas [22] has shown that the better quality of concrete surface is obtained by using concrete mixtures with higher flow parameters, but less air content. It is advantageous to use self-releasing forms for visual concrete casting as release agent tend to retard the surface causing the negative impact on physical properties of the surface [23].

Scanning Electron Microscopy (SEM) photos [9] show that different curing conditions caused different microstructure, thus the concrete of same composition may appear differently. The surface morphology (the microtexture) was observed to have a great impact on surface permeability [23].

Reitterman [23] notes that current quality evaluation methods of fair-face concrete are mainly based on monitoring of visible macroscopic defects on the surface, which are naturally subordinate to the way of their production. The researcher doubts that the visual parameters should prevail in evaluation of visual concrete surfaces, and explains it by the fact that high visual criteria are often achieved by sacrificing the surface resistance to negative environmental impact, thus the importance of durability in assessment is underestimated.

However, visual characteristic are irreplaceable for the classification. In the study “The

evaluation methods of decorative concrete horizontal surfaces quality” [22] three different methods were used to classify 4 classes of concrete specimens: Special (architectural concrete), Elaborate (decorative concrete), Ordinary concrete and Rough concrete. That is how surface quality is defined by guidelines of International Council for Building Research:

- First used method was according to GOST 13015.0-83 – Soviet standard that distinguishes seven groups of concrete surfaces from A1 to A7 according to biggest size of a blemish
- Second – using document CIB Report No. 24 “Tolerances on blemishes of concrete” where classification is done by providing the quantity and bubbles area in percent for each reference card
- The third was the author’s original method – “ImageJ” which categorizes surfaces based on the ratio between blemishes and all specimen’s area

2.3.1 Obtaining of an Image

In order to fully evaluate the quality of concrete surface, the gray scale should also be taken into consideration. Klovas [22] notes the gray scale property have been previously analyzed, and the biggest factor which influences the surface quality was the lightness of the environment. Also Klovas remarks that robustness of image taking process should be more researched in the future. Two method of picture capturing has been tried in the experimental part of this master thesis: scanning and photographing.

2.3.2 Discoloration during early age

Well known fact is that the higher water/cement ratio for the same type of cement results in lighter colour of the cured material [20]. The more water is present in concrete the more water will potentially evaporate from its surface before reacted with cement. Evaporated water leaves behind many fine voids in the matrix close to the surface. Lightness of the colour is connected to amount of those pores and cavities [24].

Detail of the pigmented concrete surface and its grayscale copy is shown on Fig. 4. Permanent discoloration can be observed on that photo. Sample of glossy smooth surface was taken out of the solid polystyrene mold after 48 hours, and other pieces of same concrete were placed onto that fresh surface. Such pattern was discovered few days later. Dark spotted regions were covered and remained to have original glossy texture and original darker color. While the rest of the surface made a transition to matt texture and significantly lighter color.

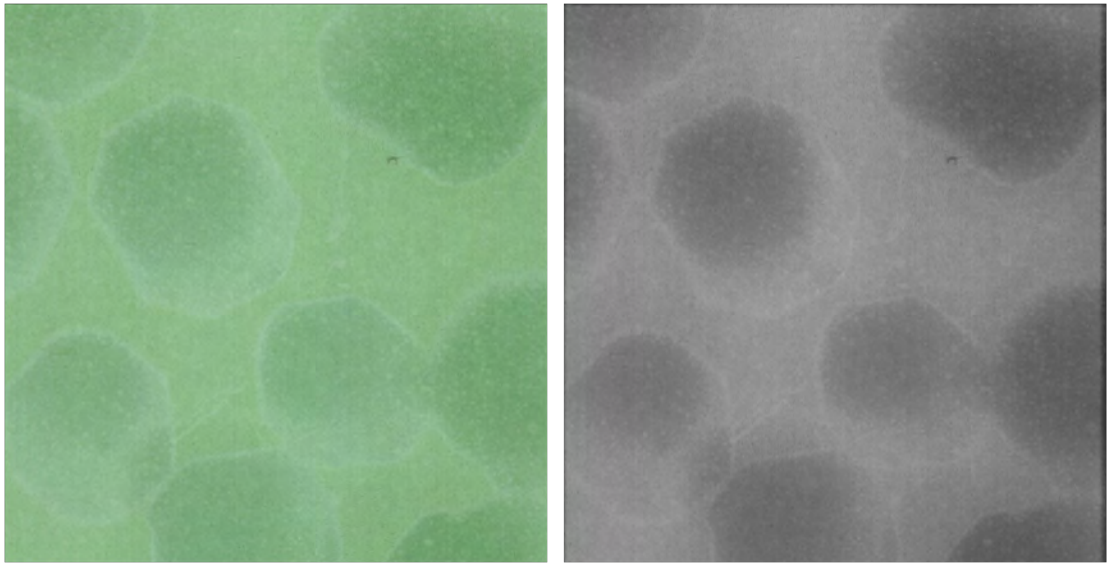


Fig. 4: Impact of uneven drying

Young concrete has faster rate of fading in color due to presence of free water therefore due to faster drying. Surface of the young concrete may change color and micro texture due to ongoing reaction and insufficient rate of hydration. When retarding admixtures are used or chemical additives have a side action of retarder for cement hydration the issue of discoloration at early age becomes more relevant. It is important not to bring visual surface of the concrete in contact with air too early. Early demolding as well as early mechanical treatment such as polishing brings greater risks of changeability of color and texture in obtained surface.

To sum up, concrete matrix changes chemically through time and respectively does its appearance. Equal curing conditions along the surface are essential not only for uniform mechanical properties of concrete but also for uniform color. Filler does not undergo chemical transition and so only color transformation of the matrix makes an impact on the overall color change. Higher amount of non-reactive aggregates exposed on visual surface minimizes the discoloration caused by escaping of water.

Same phenomenon presenting irreversible discoloration is shown on Fig. 5.

To get rid of those maps it is necessary to apply mechanical treatment such as grinding. In practice such discoloration can be omitted when mechanical treatment is the part of the project.

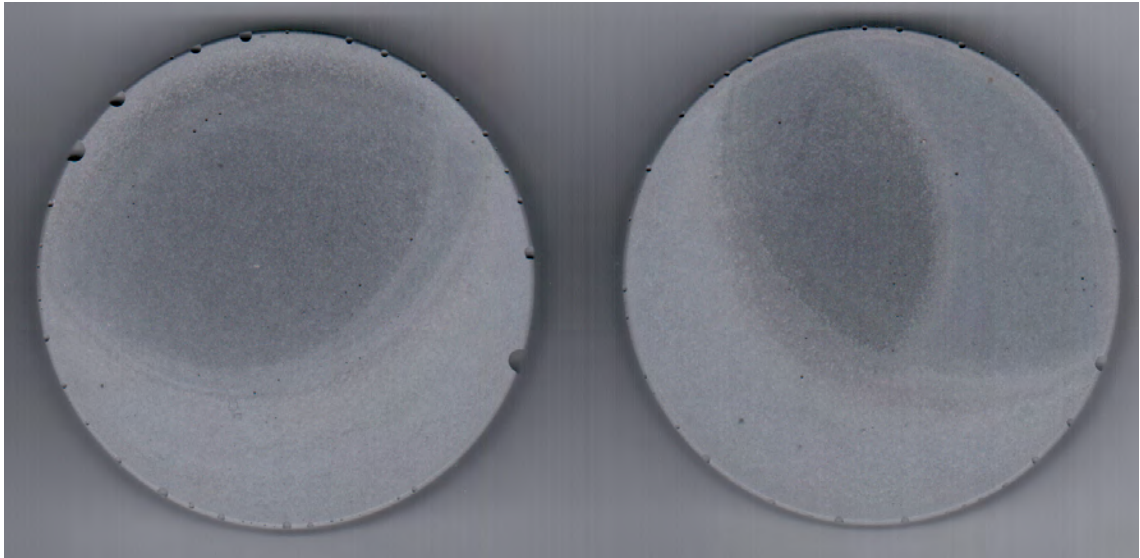


Fig. 5: Surface discoloration

2.3.3 Effect of the curing on stability of color

Is there an optimal timing for a particular mix to be kept curing inside the formwork that will grant a stable color after un moulding? Is there a recommended duration of treatment that minimizes risks of discoloration or texture change which may be caused during storage of a decorative element? To answer that question following experiment was created.

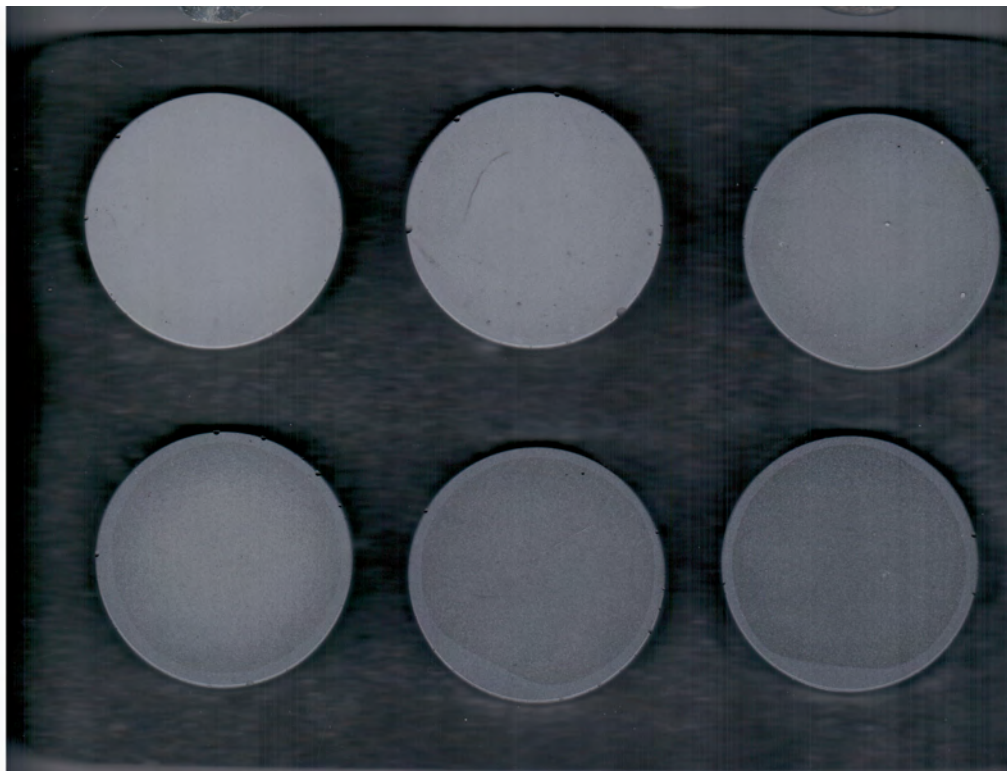


Fig. 6: Sample of the image data

The form was designed in a way that six parts of the panel could be unmoulded separately. Six surfaces of the circular shape belong to one cast (same mortar mix was used as one studied in experimental part of the thesis). Surfaces had been unformed gradually one by one in six days. The panel was repeatedly scanned in resolution 300 dpi several times after each newly unformed surface. One of the image data files which had been used for data processing is shown on the Fig. 6. Immediately after releasing from the form all the surfaces appear in the same very dark color (level of brightness intensity 42), thus several data images were obtained with 12 hours delay (see Tab. 2) in order to let the surface “dry”. Therefore the beginning of measurement of the color always started with half a day delay. Scanning took nine days and next images were obtained after larger time intervals, on 38th and 75th day.

Chronology	Surface unformed	Duration of treatment [days]	Collection of image data
0	Casting of the panel		
1 st day			
2 nd day	#1	2	scanning
3 rd day	#2	3	scanning
4 th day	#3	4	scanning
5 th day	#4	5	scanning
6 th day	#5	6	scanning
7 th day	#6	7	scanning
8 th day			scanning
9 th day			scanning
38 th day			scanning
75 th day			scanning

Tab. 2: Chronology of data collection for experimental study of effect of curing duration on a final color of concrete

In order to trace rate of color change Image Analysis Toolbox was employed to develop algorithm in Matlab. For each surface following sequence was applied within each cycle in order to numerically evaluate the tone:

Converting RGB image file to grayscale image

Distinguish borders of objects

Positioning of the centroid of an object

Cutting out a central portion of the object of a set radius

Definition of a dominant color/intensity level for that portion

Detailed analysis has been done to data obtained on 38th day. Ten scans have been used for image analysis in order to understand how it is better to work with image obtained from scanner. There are three built-in functions that may be used working matrix of pixels:

- `mean()` – returns average value
- `median()` – returns middle value
- `mode()` – returns most frequent value, peak of the distribution

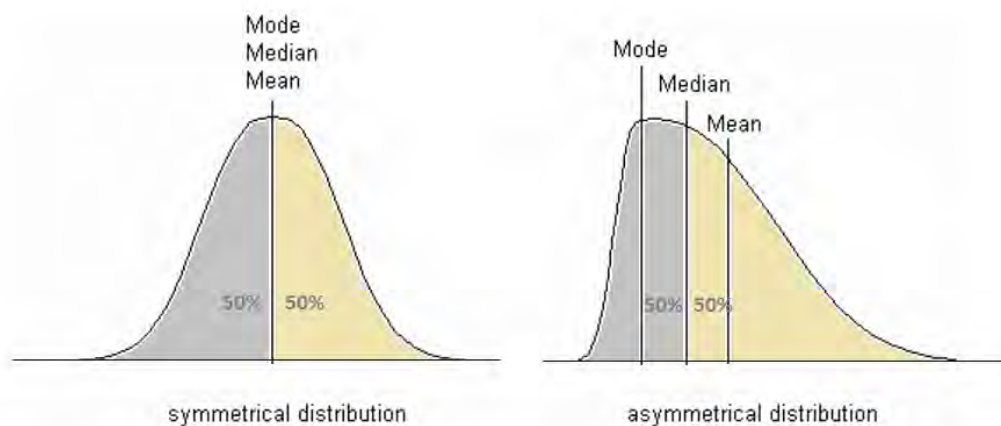


Fig. 7: Illustration of mean, median and mode values

Checking the histogram of fragments of surfaces it can be said that the distribution is nearly symmetrical, and more likely to be unimodal – having one peak value. Therefore mean, mode and median values are found very close to each other, and it is not obvious which prescribes the image better, and all of them were tested in order to define dominant intensity level. Defects such as bubbles that occupy very small areas have smaller effect on the median value and completely neglected when mode value is used. Mean value is more sensitive to the presence of bubbles on the surface.

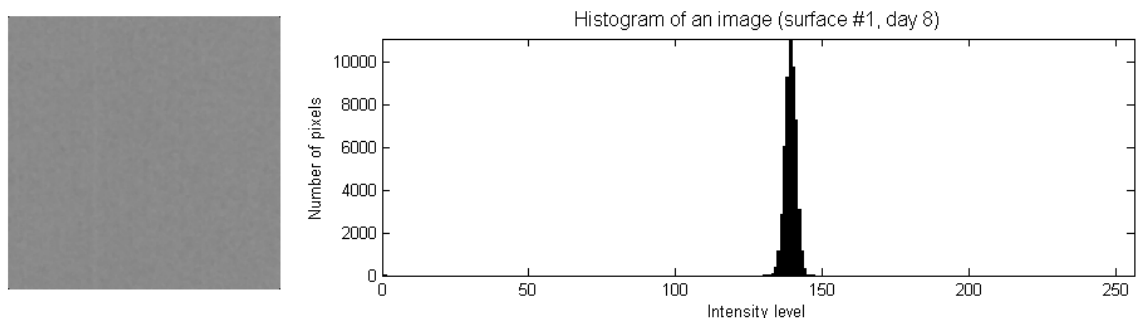


Fig. 8: Typical histogram of a light color shade

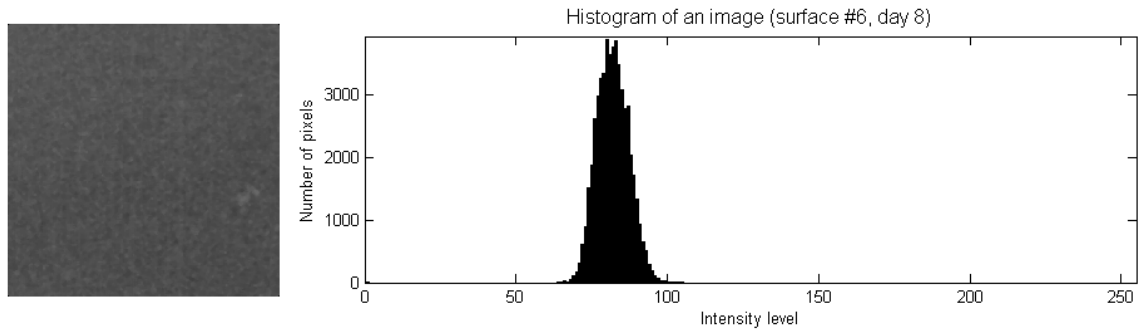


Fig. 9: Typical histogram of a dark color shade

It was observed that three values are in fact very close and the distance between them never exceeded 2.0 for the same histogram, for example, mean = 125.58, median = 126, mode = 127. 3-4 intensity levels still are not noticeable for a human eye. The difference in 7-10 levels is already apparent especially when displayed next to each other.

Radiuses of 200, 250 and 300 pixels approximately correspond respectively to 40%, 60% and 90% of a surface that is taken into account. Evaluation for 100% of the surface area is not suitable due to light stripe along the perimeter as can be seen in the detail (Fig. 6). Each bar on the chart below (see Fig. 10) illustrates the median value of measurements obtained from 10 scans. Therefore, scans with defects have the smaller effect on resulting value.

After the analysis of the obtained values, the question arose: which parameters show the largest differences between surfaces #1 to #6? The smallest differences were observed for the average value computed on the smallest area. The largest differences were found for the mode value in combination with the largest area.

It is also can be seen that increasing of the area upon which the color approximation is done leads to darker result tone regardless of the employed function. Towards the center of the surface the tone gets lighter, that can be viewed directly from the image (Fig. 6), that effect is the most apparent for surface #4.

It seems that function mode() and radius of 300 pixels will be useful for analyzing tone differences between surfaces for particular panel scanned in 300 dpi resolution. Those parameters were used to processed data from 2nd till 9th day and 75th day.

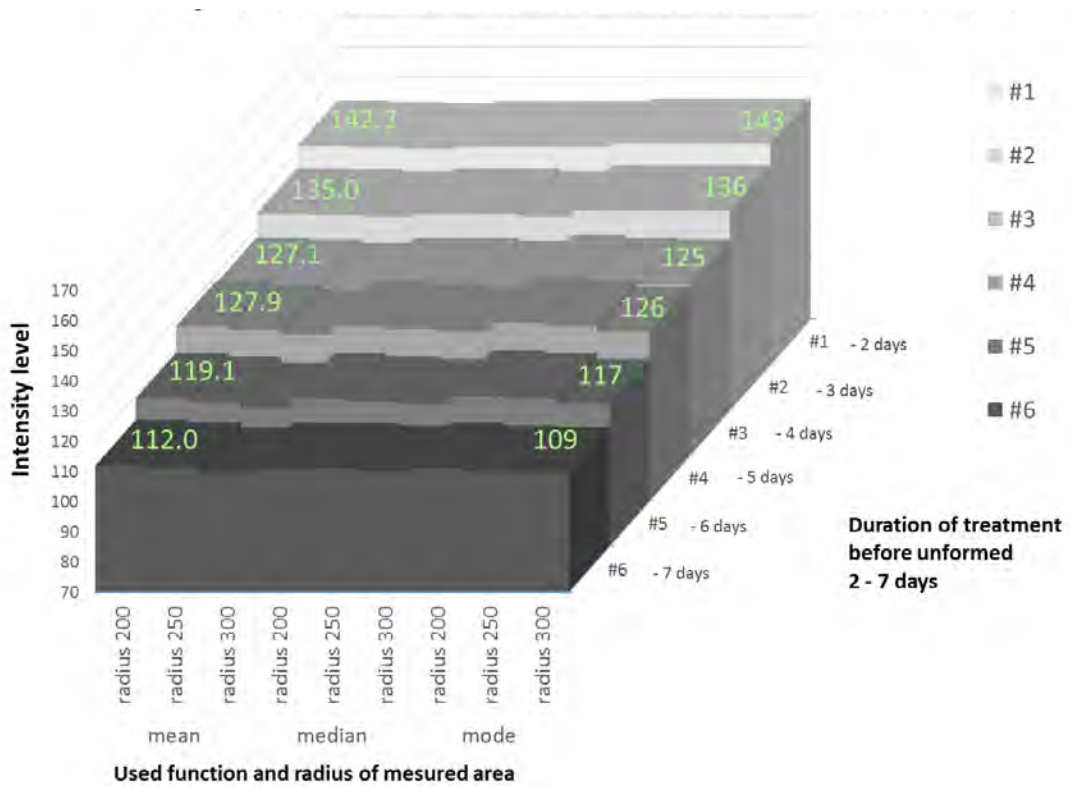


Fig. 10: Intensity levels on grayscale 0-255 measured on 38th day for surfaces with different duration of treatment

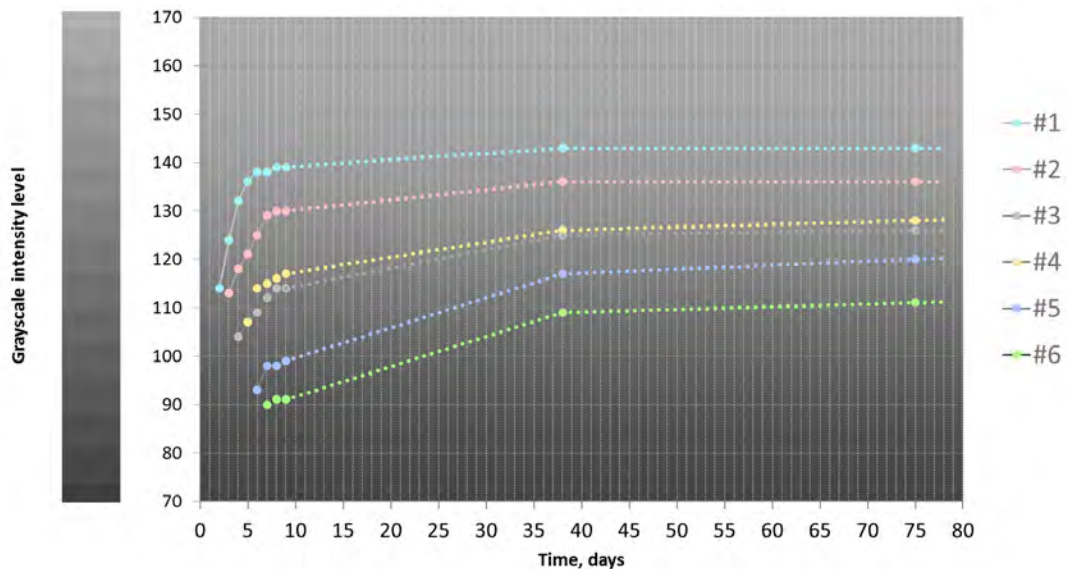


Fig. 11: Color transition throughout time

Following experiment shows that the final color is not solely affected by the w/c cement ratio of the mixture, but also by time for which concrete surface is kept in airtight formwork, or formulating more generally the time for which evaporation of the mixed water from a surface is prevented.

Differences in 6 days of duration of curing in the form resulted in 30-34 levels of brightness intensity for the particular HSM mix. Depending on lighting conditions 30 levels (scale 0-255) are very well distinguished by human eye:



Fig. 12: Brightness transition for surfaces #1 - #6 with assigned values

When unformed after staying in mold for 7 days the brightness change is not that rapid in comparison with change that earlier unmolded concrete exhibits. It is not correct to state that 7-days treatment duration ensures stable color tone, however it results in permanently darker tone of the surface. The lighting of the gray shade occurs after all durations of treatment.

Most important is to avoid any manipulation with the form containing young concrete. Even small pressure applied to the mould leads to separation of concrete from the mould's walls and opens the path for the air entry. Loss of contact also happens due to shrinkage of the hardening mixture. The shrinkage should be estimated and taken into account. When not prevented it is beneficial to release visual surface sooner and to switch to air-curing.

3 OBJECTIVES

The experimental investigation is assumed to go through following stages:

Preparation of the samples

Implementation of series of tests

Comparison of the surface samples for their

- capability of water penetration reduction
- capability for maintaining the visual characteristics after chemical damage
- ability to withstand abrasive load

Quantification of degradation by using visual methods

Evaluation of the effectiveness of surface treatment

Discussion of applicability of studied surfaces

4 EXPERIMENTAL INVESTIGATION

4.1 Mix design and preparation

Desired reduction of ingress of aggressive substances may be done by efficient particle packing of the mixture. Utilization of that approach also allows mechanical strength increasing favourable for abrasive resistance of decorative concrete. Enhanced workability broadens the possibilities for mixture applicability.

4.1.1 Mixture proportions

The recipe of HSM was assembled by using EMMA (Elkem Mix Material Analyser). EMMA is a freeware that calculates and displays the particle size distribution (PSD) of a mixture of components. Program was developed at the company Elkem and was adopted to examine PSD of a combination of materials of different building products including concrete. Knowing the PSD for input materials it is possible to specify the distribution for any combination of these materials. After the quantity of the individual materials has been entered, the PSD of a mix is presented in a form of graph [25]. The Andreassen model (1931) of an optimal packed mix was applied for efficient particle packing. The model is represented by a straight line in cumulative double-logarithm diagram of PSD [26]:

$$CPFT = [d/D]^q \quad (1)$$

where

CPFT – Cumulative Percent Finer Than (volume)

d – Particle size

D – Maximum particle size

q - Distribution coefficient (q-value)

User specifies q-value, size of the largest particle of the mix, and PSD of constituents. Interesting and informative points are given in program guidelines regarding distribution coefficient specification. User guide states that there is no hard correlation between the q-value and rheological properties; however, q-value sets the slope of the straight line (red line on Fig. 13), thus

- The higher the q-value, the coarser and less workable the mix is
- At lower q-value, the fines content is increased and the mix is more workable
- Good free-flow in mortar results when the q-value is less than 0.25

- For self-compacting concrete 0.28 has been found beneficial

Precise granulometry measurements of all constituents were outside the scope of the thesis thus some deviations from actual PSD of used materials are possible. The grading of the sand and the granulometry of the limestone dust were adopted from producer’s technical list (Appendix B) and then exported to the program. Portland cement with a specific surface area (SSA) of 375 m²/kg was used. Detailed granulometry curve of the same grade of Portland cement was found and adopted from [27]. Its chemical compositions can be found in Appendix X. Materials such as MS and FA are varying significantly from supplier to supplier. In the case of fly ash input values were derived based on typical PSD of such material obtained from [28].

CEM I 42,5 R SSA = 375 m ² /kg		Fly ash		Microsilica SSA = 21 m ² /g	
Size [μm]	Typical [%]	Size [μm]	Typical [%]	Size [μm]	Typical [%]
<200	100	<200	100	<2	100
<90	99	<100	97	<1	99.8
<63	95	<62	80	<0.5	92.9
<45	85	<44	72	<0.32	83.5
<30	67	<31	59	<0.2	65.6
<20	51	<22	49.3	<0.16	52.1
<10	30	<11	32.6	<0.12	31
<5	16	<5.5	18	<0.1	24.6
<1	4	<4	11.5	<0.08	13.8
<0.5	1.7	<1.6	2.5	<0.063	6.4
<0.2	0.3	<0.8	0	<0.04	0.11

Tab. 3: Particle size distribution for selected constituents

Afterward a suitable combination of the constituents was looked for that makes the closest fit to the Andreassen model. Chosen distribution value is $q = 0.26$. It is very important to provide very high workability for such mix therefore:

- Reduce amount of trapped air, minimize size and amount of open bubbles on the visual surface.
- Recruit self-compaction mechanism favourable for achieving dense and less permeable mortar matrix, approach desired particle packing without vibration.
- Ensure that mixture is suitable for placing in well detailed forms, is able to display fine decorative detailing, and thus fulfills functional requirements.

Optimized mixture recipe and PSD obtained in EMMA are displayed below (Tab. 4 and Fig. 13).

Following steps toward packing improvement can be done by integration of the ingredients with 1-2 microns average size grain and addition of finer filler with grains mostly in size of 100 micron.

Self compacting mixtures requires high paste volume. When the suspension of filler in paste increases, the workability of the mix will increase. The thickness of the paste layer surrounding each aggregate particle determines the degree of workability and is closely related to the surface area of the aggregate. When developing Micro Mortar Optimization Applied on Self-Compacting Concrete Utsi [29] applies recommendations that the coarse aggregate should not exceed 50% of the solid volume because a high volume of mortar is important to prevent blocking. Also that the fine aggregate content shall be 40% of the total mortar volume.

Cement content remains very high although is lowered by supplementing cementitious materials. Designed mix resulted in 12.5%, 11.5% and 15.9% cement replacement by mass by LS, FA and MS respectively. Such high amount of powder will not entirely contribute do the binding function. Part of the powder volume namely limestone dust was taken and further on treated as fine filler.

Component	Description	d50 [μm] in EMMA	Density [g ml ⁻¹]	Proportion EMMA	mass in m^3 [kg]		
Silica sand	STŘELEČ - ST 01/06	437.77	2.65	44	1157	filler	50%
Limestone dust	D8	58.12	2.4	9	194		
Portland cement	Českomoravský cement CEM I 42.5 R	19.74	3.16	25	934	binder	50%
Fly ash		22.61	2.3	9	178		
Microsilica	SIODIX	0.16	2.25	13	246		
				100	2710		
Superplasticizer	STACHEMENT 2180				40.8		
Water admixed	potable				352.0		
Water total						380.5	
price for m^3	8087 CZK						
SP/binder	3.00%						
water/binder	0.28						
binder/filler	1.01						

Tab. 4: High strength mortar mix recipe

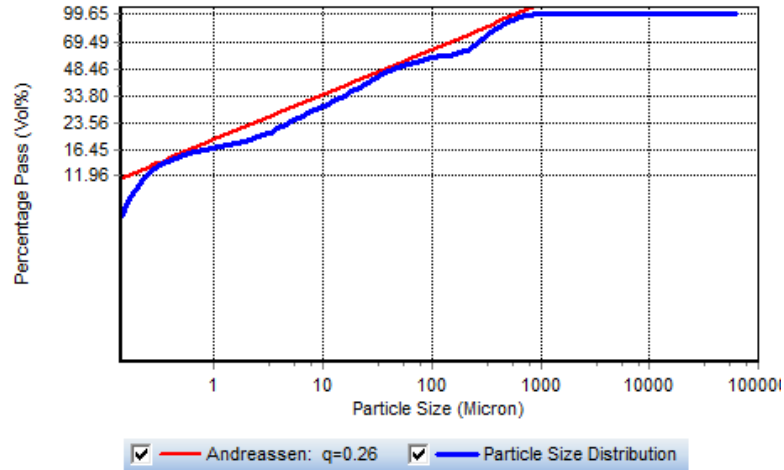


Fig. 13: Particle size distribution curve of proposed HSM

Plain Portland cement mortar (PPCM) has been mixed as the reference mix (see Tab. 5).

Component	Description	Density [g ml ⁻¹]	Proportion	mass in m ³ [kg]		
River sand	0-4	2.65	77	1954	filler	70%
Portland cement	Českomoravský cement CEM I 42.5 R	3.16	23	830	binder	30%
			100	2784		
Water admixed	potable			373.5		
Water total				373.5		
price for m ³	2075 CZK					
SP/binder	0.00%					
water/binder	0.45					
binder/filler	0.42					

Tab. 5: Plain Portland cement mortar mix recipe

The material costs for SCC is in general higher than ordinary vibrated concrete because of the increased amount of cementitious materials, fine fillers and high-performance superplasticizer [29]. Calculation of prices of particular mixes confirmed a great (almost 4 times) cost increase for the highly workable HSM.

4.1.2 Mixing procedure

Mortar was mixed in the ALBA HOŘOVICE Mixing Machine RE 24 in 30 l bowl. Great amount of fines in the mixture requires special attention to duration and energy of mixing. It is important that all particles especially the very fine ones, are uniformly distributed. Silica fume tends to form agglomerates, the minimal shear force for breaking this agglomerates can be reduced by keeping the particle dry; thus it is recommended to mix all dry particle before adding the water [30]. Pauses are necessary for manual checking of homogeneity of the mix, breaking of lumps and clots, and scraping parts of the mix stuck to walls of the bowl. For the adopted procedure see Tab. 6.

“dry mixing”		speed 1	2 min	Dry components are mixed with 50 g of mixed water
	pause	-	1 min	
		speed 1	2 min	
“1/2 water”		speed 1	2 min	Mixing with half of the rest of water gradually (first 30 sec) added to the bowl
	pause	-	1 min	
		speed 1	2 min	
“1/2 water + SP”		speed 2	5 min	Rest of the water mixed with superplasticizer gradually (first 30 sec) added and mixed
	pause	-	1 min	
		speed 2	5 min	
Total time			21 min	

Tab. 6: Mixing procedure

Forms for samples were filled with designed mixture without compaction of the material. As well as no vibration was applied filling tree gang prism molds for further testing of flexural and compressive strength. Ordinary concrete mixed due to very low slump required compaction to fill the forms.

4.1.3 Curing regime

Duration of curing depends on few factors, such as desired strength and durability of concrete, its size and geometry, requirements on plastic shrinkage prevention. As it was described earlier in order to minimize possible discoloration of surfaces the curing was prolonged up to 7 days. Samples were cured in ambient laboratory conditions: RH 35% and 23 °C. Fresh mortars hardened under the lids of Petri dishes which are not airtight and allow air circulation into the form at the same time protect mixture from excessive

evaporation. Prisms were stored in same ambient conditions covered with plastic foil but not fully wrapped.

4.1.4 Basic physical properties

Haegerman’s mini cone for mortar was adopted for measurement of fresh properties of the mixtures; however flow test was not performed according to ASTM C1437 (Standard Test Method for Flow of Hydraulic Cement Mortar). The mixture was not given specified tamping for compaction when filled in the cone. Flow was measured without compaction drops. Three measurements of the self-weight flow on a glass plate gave a value of 32 cm with absolute absence of bleeding, what together ensure dynamic and static stability of the mixture.

	Plain Portland cement mortar (PPCM) Reference mixture	High strength mortar (HSM) Non-compacted studied mixture
Mini slump flow [mm]	0	320
Visual Stability Index according to [31]	1 - stable	0 - highly stable
Flexural strength/St. dev [Mpa]	7.03/1.36	6.42/1.75
Compressive strength/St. dev [Mpa]	49.17/4.37	76.46/5.06
Bulk density/St. dev [kg/m ³]	2157.0/32.9	2117.9/12.3
Effective porosity [-]	0.211	0.151
Saturation at the beginning of surface absorption test	34%	73%

Tab. 7: Basic physical characteristics of studied mixtures

During abrasive wear test it was observed that HSM samples kept releasing water vapor around 28th day. This evidences about yet imbalanced hygral state of the sample in ambient conditions of 35% relative humidity. The rate of the weight reduction was approximately 0.03 - 0.09 g/day (varied for different samples). Taking into account mass of the sample this is corresponding to 0.025 - 0.08% weight loss per day. The fact relates well with the higher saturation (around 75%) of the HSM samples that was later discovered, when measurements of mass of fully saturated, completely dry, and one at the start of testing were analyzed.



Fig. 14: Mini slump testing of HSM and PPCM

The compressive and bending strength of proposed mortar after 28 days as well as flow ability of the fresh mixture were slightly worse than expected. Previous testing of the mix of same composition implemented by author resulted in less viscous consistency with the self-flow of 35.5 cm. Aging of constituents may be one of the reason as it leads to agglomerates in powders that are harder to break. Physical properties are also sensitive on change of mixture volume and change of mixer what results in different amount of energy applied to mixing process. And the most relevant factor would be storage conditions of prisms before strength testing. It can be beneficial to produce concrete with water-to-binder ratio below the value of 0.4 - 0.45. However working with very low amount of mixed water requires better care regarding prevention of water loss. “Even a modest water loss might therefore cause a significant reduction of the quality compared to the quality, which could have been obtained under favourable hardening conditions” [32]. Number of experimental studies has shown that the curing conditions substantially affect the capillary permeability. Sufficient curing is essential for a concrete to provide its potential performance [9]. Importance of curing regime on sorptivity was also investigated by Tasdemir [33]. Moreover it was observed that water curing has more effect on the permeability than on the strength of concrete. Another important point has been made regarding microfiller materials with the low value of pozzolanic activity. Tasdemir observed that those microfillers exhibit very little cementing value in laboratory conditions, however, under water-curing conditions, the cementing activity becomes apparent.

4.2 Description of tested samples

Overall an untreated sample of a surface of the ordinary concrete and four variations of a surface of proposed mixed were examined. Laboratory Petri dish, a shallow cylinder made of solid polystyrene served as form for the samples. It was decided to implement minimal interference to desired surfaces as an effort towards minimization of the cost associated with treatment. Overall, chosen treatments primarily should fulfill:

- Serve an invisible protection, not to change an original surface appearance
- The sheen (when remained) is provided by surface structure not by applied coating.
- Breathable, escape of moisture is not prevented



Fig. 15: Petri dish

Explanations of sample's notations see below in Tab. 8:

U	Untreated
M	Mechanically treated
IM	Impregnated and waxed without mechanical treatment
M+IM	Mechanically treated, impregnated and waxed
UP	Untreated plain Portland cement mortar

Tab. 8: Notations of the categories of samples according to applied treatment

Thin top layer was mechanically removed by brushing with diamond pad. Further on the surface has been hydrophobized with commercially available nanoimpregnation for natural and artificial stone and porous building materials. Nano impregnation works on the principle of surface tension that repels liquid. Nano particles are uniformly penetrated (soak) into the depth of the material, but not form a continuous film. All surfaces were

saturated by submersion of the whole sample in impregnating product for 5 minutes. Excesses of the product had been removed from the surface and a sample was left air-dried for 24 hour according to producer's recommendations. Treatment of the impregnated surfaces was completed with polishing with protective varnish.

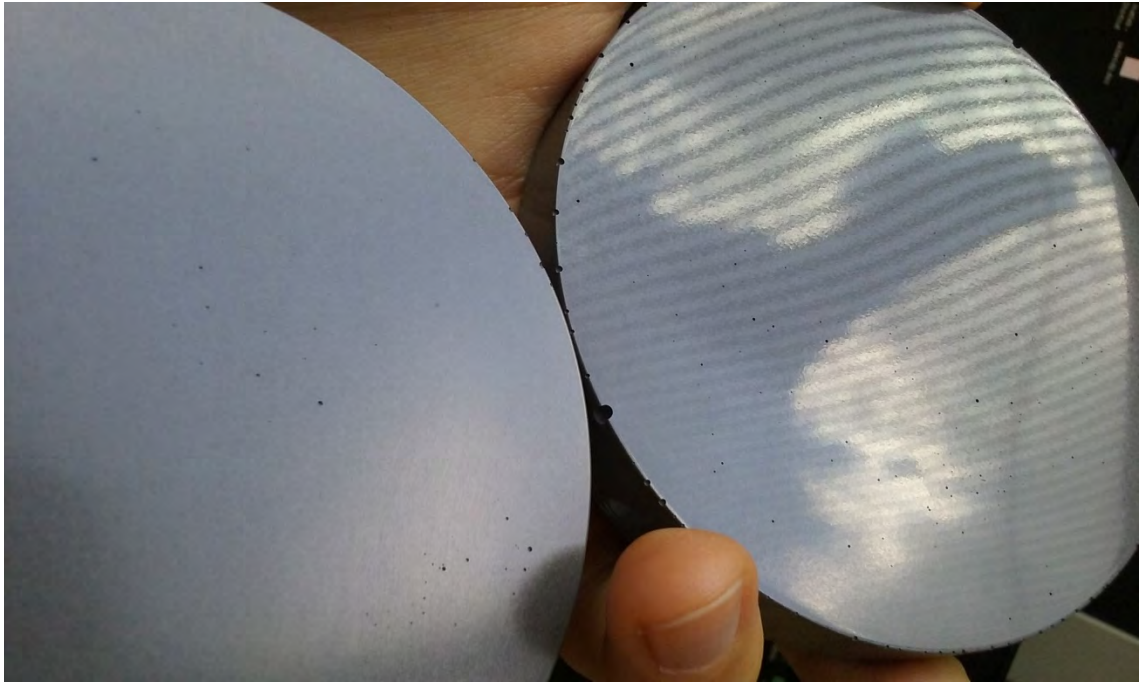


Fig. 16: Visual appearance of M (left) & U (right) treatments

4.3 Schedule of the experimental part

days	action	condition for curing/storing
0	casting of samples	curing in the lab in Petri dish
1		
2		
3		
4		
5		
6		
7	samples unformed	continued curing in their forms
8		
9		
10		
11		
12		
13		
14	mechanical treatment	period associated with varying ambient conditions
15		
16		
17		
18		
19		
20		
21	impregnation	storing in the forms
22	waxing	
23		
24		
25		
26		
27	abrasion	
28	strength measurements on prisms	samples submerged after water absorption testing
29	photo shooting of samples	
30	chemical damage	
31	abrasion	
32	photo shooting of samples	
33		
34	abrasion	
35	surface water absorption test	drying in the oven
36	abrasion	
37	abrasion	
38	abrasion	
39		
40		
41	abrasion	
42		density and porosity specified
43		
44	abrasion	
45	abrasion	
46	density and porosity specified	

Tab. 9: Schedule of experimental part

4.4 Water absorption test



Fig. 17: Arrangement of the surface water absorption test

One of the ways how water is transported into a material is by capillary forces in the liquid state. Decorative or interior concrete surfaces usually exposed to liquids cyclically, not permanently, rarely being submerged, exceptionally exposed to water under pressure. Measurements of vertical unidirectional uptake were found suitable and sufficient means for estimation differences in water absorption of studied surfaces. In [34], it has been shown that there exists a relation:

$$i = i_0 + At^{-0.5} \quad (2)$$

which also typically fits tests which directly measure the rate of capillary sorption CAT (Covercrete Absorption Test) and the ISAT (Initial Surface Absorption test) [35],

where

A – Water absorption coefficient [$\text{kg m}^{-2} \text{s}^{-0.5}$]

i – Mass of water per unit material surface that is in direct contact with water [kg m^{-2}]

t – Time of the contact with water [s]

Divided by density of water ρ_w the relation is also met in form:

$$I = C + St^{-0.5} \quad (3)$$

where

S – Sorptivity [$\text{m s}^{-0.5}$]

I – Cumulative water uptake [m]

C – Initial disturbance observed by some researchers and it is believed to be dependent on the surface finish [34] or correction term added to account for surface effects [34]

Dependence of sorptivity values S obtained during testing on the moisture condition of a specimen prior to testing is mentioned in many sources [36], [37], [35]. It is known that absorption is not related solely to the structure of pores. The higher the moisture content of the concrete the lower the measured sorptivity. A linear trend was found by Nokken and Hooton [37] relating normalized sorptivity values to initial degree of saturation. It is recommended to condition specimen at 105 °C before measuring; otherwise, it is important to establish the hygral state. It was not known how high temperatures may affect products applied on the surfaces, and the impact of surface treatment is the point of interest for the study. Therefore, it was decided to implement testing on specimens conditioned in ambient laboratory conditions at a standard relative humidity and temperature of 23 °C.

For a particular set of specimens the following consequence was chosen: induce a consistent moisture condition in the capillary pore system, complete water absorption testing, achieve state of 100% saturation, proceed with complete drying of samples in ventilated oven at 105 °C, and based on measured data with retrospective calculation obtain original hygral state (see section 4.3).

4.4.1 Results interpretation

- The function of water inflow versus square root of time of U, M, IM and M+IM samples after a certain time period exhibit nearly same slope of linear increase. That is an evidence of characteristic that does not depend on variances in surface structure; same material exhibits same sorptivity. Factors that mainly influenced the amount of absorbed water are hidden earlier and can be well distinguished during first 10 minutes of the test.
- Also, the radical difference can be seen between water permeability rates of UP-samples made of mortar mixture with plain Portland cement and the rest of samples. Water inflow of untreated UP-samples is about 5 times higher than one of the U-samples of proposed mortar mix.
- Based on obtained values it can be seen that before the 5th minute the removal of the laitance of the M-sample leads to smaller absorption comparing to an untreated U-sample, but between 5th and 10th - minute surfaces already exhibit nearly same water inflow. Time interval 2 - 5 minutes is the best for the presentation of variance among all treatments.
- The disadvantage of the used testing method is in an insufficient accuracy of measurements taken up to one or two minutes. Errors appear when measuring the surface which was wetted but the water did not penetrate into the surface structure, or when absorption increment was too small – less than 7 g/m². Therefore, measured data are in the strong dependence of how well water drops have been wiped off before sample was weighted

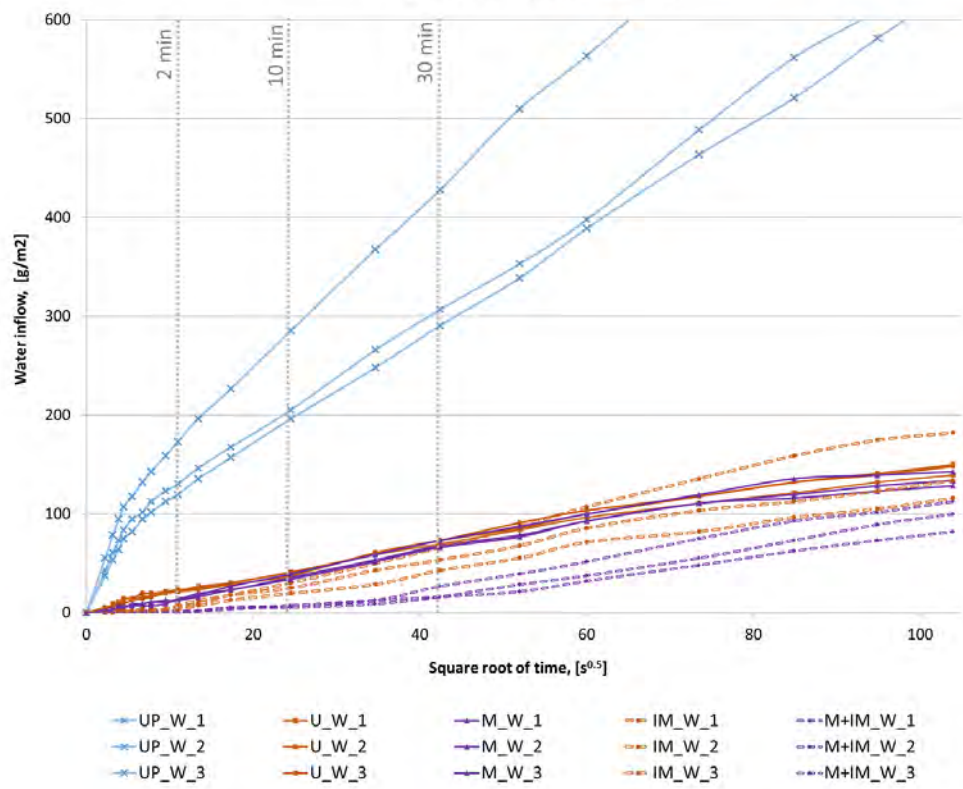


Fig. 18: Vertical water uptake - 3 hours

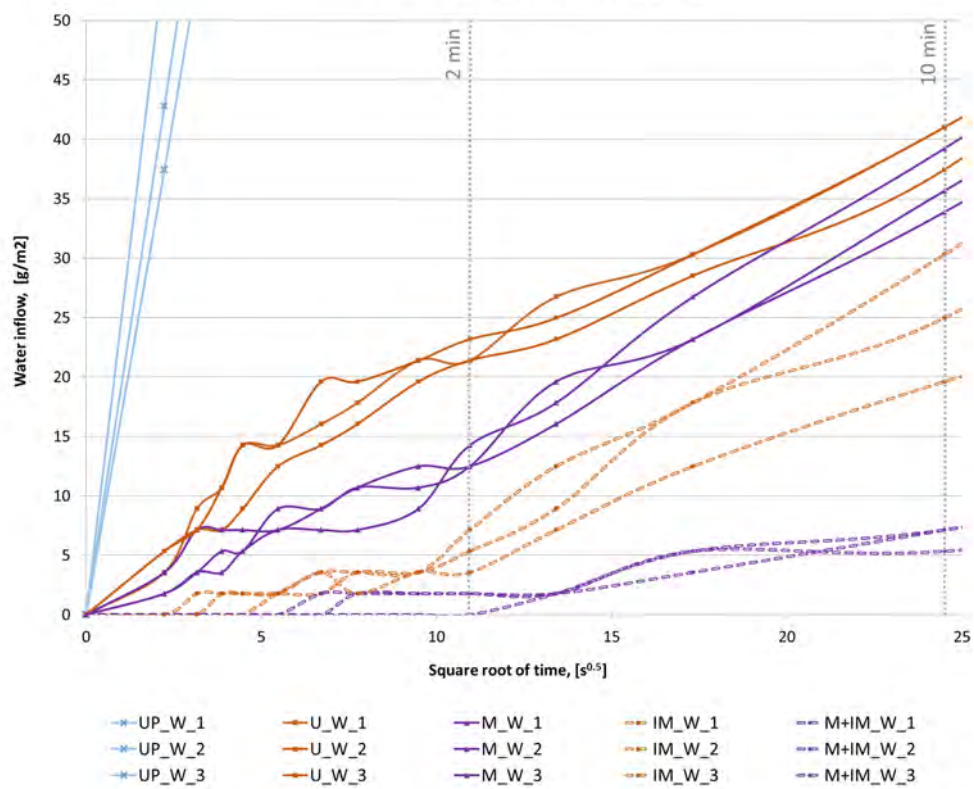


Fig. 19: Vertical water uptake - 10 minutes

- For surfaces protected with impregnation, the beginning of absorption is considerably postponed. Time when water starts to get through with the same rate as samples without impregnation can be estimated as:
 - 2 minutes for samples IM
 - 10 minutes for samples M+IM

The importance of surface preparation for efficient use of hydrophobizing agent becomes obvious after analysis of the data presented on the graph.

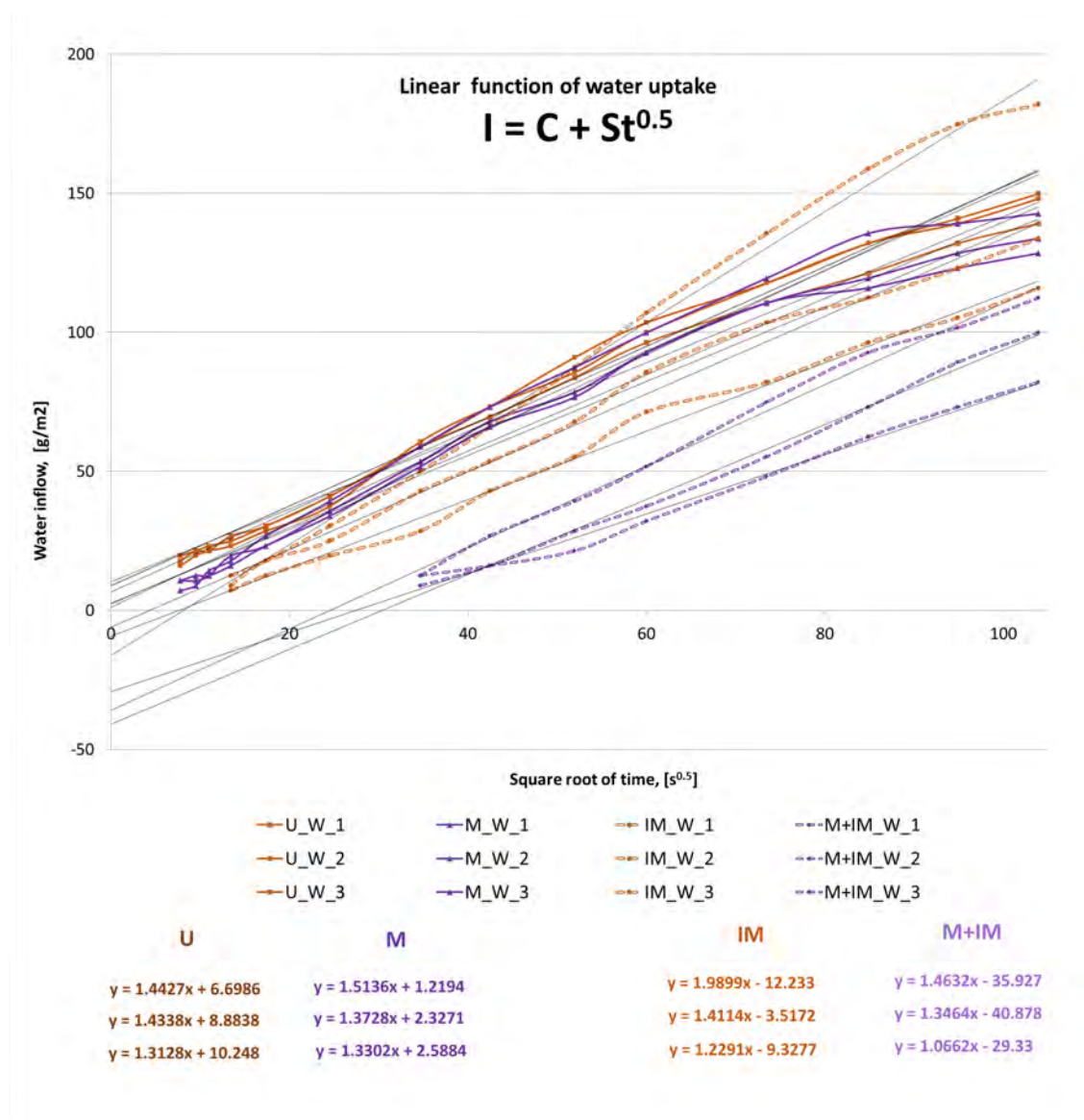


Fig. 20: Trendlines of vertical water uptake

Using linear trendline it is possible to evaluate the sorptivity S for all U, M, IM and M+IM samples. S-value was also computed for UP mix. The evaluation of disturbance C is outside the scope of this master thesis.

4.4.2 Comparison of results

Parameters are summarized below in Tab 10, average sorptivity equals to 1,414 kg/(m² s^{1/2}). Is this value in a good agreement with the measurements reported by other researchers?

		S [kg/(m ² s ^{1/2})]	Degree of saturation [-]
UP	1	7.9788	35%
	2	5.9305	
	3	5.6766	
Average		6.5283	
U	1	1.4427	
	2	1.4338	
	3	1.3128	
M	1	1.5136	73%
	2	1.3728	
	3	1.3302	
IM	1	1.9899	
	2	1.4114	
	3	1.2291	
M+IM	1	1.4632	
	2	1.3464	
	3	1.0662	
Average		1.414	

Tab. 10: Sorptivity values obtained from water uptake trendlines

There are fewer studies devoted to interaction of two and more of supplementing cementitious materials. Fly ash and silica fume can be valuable tools in reducing permeability. These advantages vary with the type of cementitious material. It seems that analysis of combination of alternative cementitious material. Current mix includes LD, FA and MS all in high volumes what makes it outstand among high performance mortars.

Low permeability concrete is proposed as one that has the value of sorptivity lower than 0.1 mm³/(mm² min^{1/2}) in article devoted to near surface characteristics of concrete containing supplementary cementing materials [38]. Average sorptivity of the mortar of current study after conversion of units equals to 0.01096 mm³/(mm² min^{1/2}).

Durability characteristics of HPC containing other type of pozzolan – metakaolin - was studied in Czech Technical University [39] The use of metakaolin in Portland cement-based composites as an alternative material to silica fume also contributes to refinement of pore structure. Maximum aggregate size used for that mixture containing Czech metakaolin was 16 mm. Water absorption rate of such mortar exceeds 0.0070 kg/(m² s^{1/2}) what is

more than 5 times higher permeability in comparison with $0.0013 \text{ kg}/(\text{m}^2 \text{ s}^{1/2})$ derived in current research. For more details see Table 10:

A wide range of mixes has been tested within research [12] focused on influence of aggregate gradation, cement content, silica fume content (from 0% to 25%) and super plasticizer dosage (from 0.0% to 3.5%) on durability of HPC. HPC mixes has been proportioned in the way to achieve effective particle size distribution with maximum grain size of 20 mm.

Recommendation of that study was to use, cement content in the range up to $525 \text{ kg}/\text{m}^3$ with MS content of about 10% and SP dosages of about 2% for developing flowable HPC mixes with negligible water absorption. Detailed results are shown for mixes that had $450 \text{ kg}/\text{m}^3$ of cement and water/cement of 0.23. Sorptivity values of those mixes varied between 0.0167 and $0.0552 \text{ mm}^3/(\text{mm}^2 \text{ min}^{1/2})$; and compressive strengths are within interval 80.5 - 112 MPa. Mixture presented in that work has lower sorptivity values even though w/c ratio is higher and microsilica dosage exceeds recommended 10% [12]. The lack of information about hygral state of measured samples, absorption properties of used filler and other information complicates the comparison. Nevertheless summary of several mix characteristics are given in Table 11 for the image of numerical values of sorptivity in high strength mortars:

Sorce of mix	Cement content, $[\text{kg}/\text{m}^3]$	w/c	Ultra fine powder content, [-]	Super-plasticizer dosage, [-]	Sorptivity, $[\text{mm}^3/(\text{mm}^2 \text{ min}^{1/2})]$	Compressive strength, [MPa]	Maximum grain size, [mm]
	934	0.28	15.9%	3.0%	0.0110	76.5	0.6
	830	0.45	-	-	0.0482	49.2	4
[12]	450	0.23	20%	3.0%	0.0458	111.0	20
[12]	450	0.23	15%	3.5%	0.0292	83.0	20
[12]	450	0.23	15%	3.0%	0.0252	95.0	20
[12]	450	0.23	15%	2.5%	0.0278	108.0	20
[12]	450	0.23	10%	3.0%	0.0236	98.0	20
[39]	440	0.293	10%	1.10%	0.0543	85.9	16
[39]	484	0.293	-	1.10%	0.0768	85.2	16

Tab. 11: Characteristics of mixtures with high share of SCMs

4.5 Chemical attack test

As it was mentioned earlier alkaline cementitious materials are subjected to considerable levels of acidic agents in different fields of application. Generally speaking, any fluid that

has pH value lower than pH of hydrated cement (around 13.0 - 12.5) causes reduction of the alkalinity of hydrated cement, therefore consequently leads toward destabilization of products of hydration as it penetrates the pore structure. The most potentially aggressive environment for a visual concrete indoors are spaces for cooking, area near kitchen countertops, stove and sink. Unsealed concrete particularly sensitive to acidic liquids such as lime juice, wine or vinegar, which not just leave stains but roughen the texture as result of reaction with highly alkaline cement paste and dissolution of the surface. Other substances such as grease and oil are less harmful for the texture although result in evident discoloration.

In the scope of this experiment 12 household liquids were tested for the effect on visual appearance of the surface.

Product	pH
#1 Cleffect - abrasive cleaner	~ 13.0
#2 Water	~ 7.0
#3 Black coffee	~ 5.0
#4 Dark liqueur	~ 4.0
#5 Hand cream	~ 5.0
#6 Pumpkin seed oil	~ 4.6
#7 Soy sauce	6.0-6.6
#8 Vinegar	~ 3.0

Tab. 12: Substances used in chemical attack testing

Six isolated rectangular regions were prepared on each surface using impermeable paper tape. This allowed testing the action of two products on each sample; every substance was tested for three different durations. The arrangement of the test is depicted on Fig. 21.

1. Product was applied on the clean dry surface completely covering the relevant region, applied with excess, but not overflowing in case of liquids (see Fig. 22)
2. Product was left to act in ambient conditions
3. Rest of substance was removed with dry cotton pad
4. Affected area was lightly scrubbed with wet in water clean pad
5. Finally, region was rinsed with water and blotted dry with clean paper tissue.

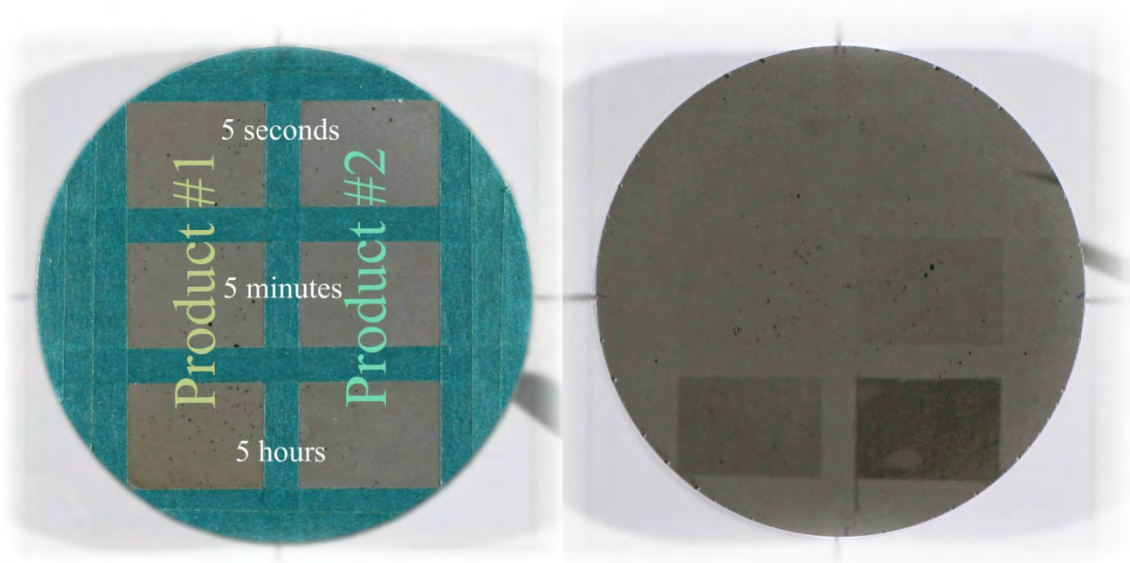


Fig. 21: Arrangement of chemical attack test

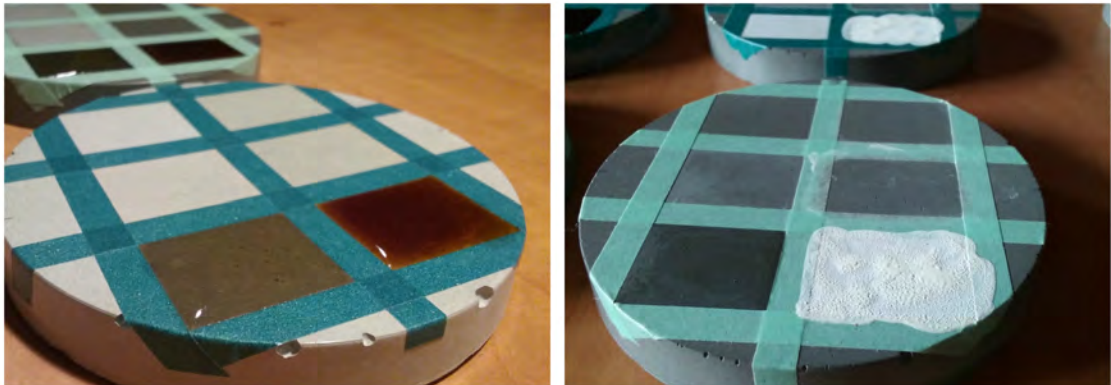


Fig. 22: Application of tested substances onto surface samples

In this experiment image data were obtained by digital camera. Photographing in photo studio allowed providing constant lighting conditions before and after the appearing of the stains. Symmetrical arrangement of identical flash lights and camera fixing on the stand above the target with photographed samples were kept the same. Standard GS gray calibration card accompanied with software provided a tool for calibration of neutral gray tone, therefore, balancing of RGB channels of colourful image.

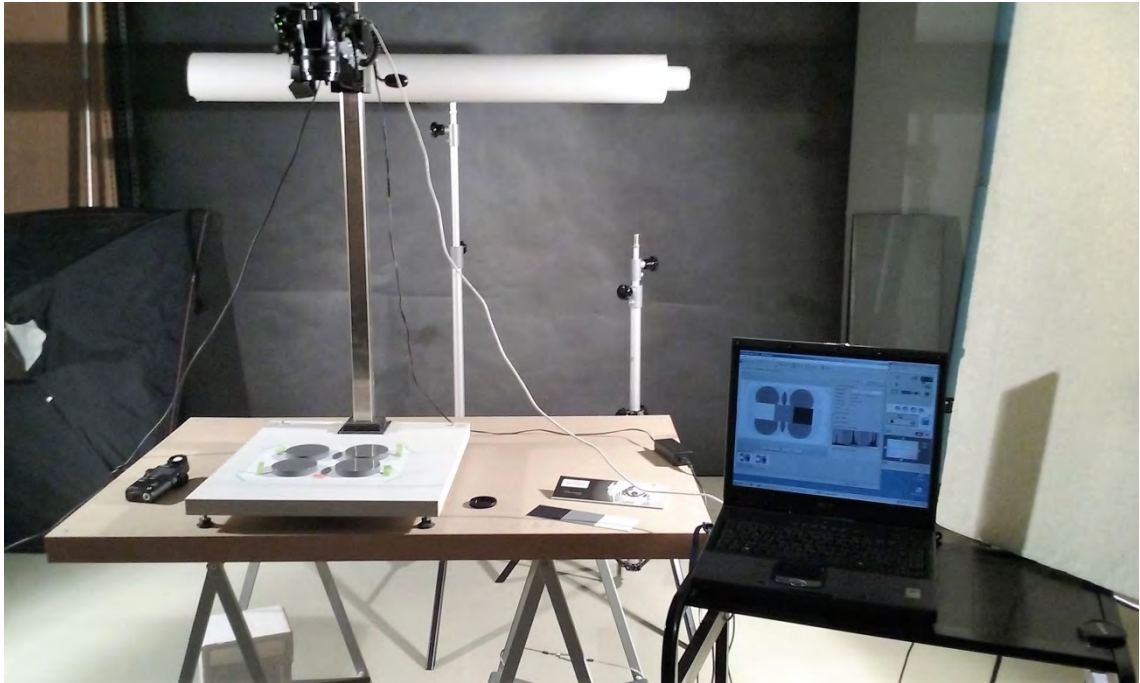


Fig. 23: Photo studio setup for collection of image data

In order to determine changes of the examined surfaces, it became necessary to develop an algorithm for processing the image data of samples.

4.5.1 Image processing

The developed Matlab algorithm allows image segmentation, calculation of parameters (attributes extraction), brightness calibration and composition of a new image, previewing and visualization of data. Complete code in Matlab with comments can be found in Appendix C.

It was observed that even in a studio shooting it is hard to achieve identical images in terms of brightness taken one by one. Revising the picture duplicates a slight variations in brightness intensity were detected. To eliminate that problem the fragments of the background were adopted as calibration elements. On the picture below where the mask applied those elements are the four longer rectangles. Background (the sheet of paper underlying the samples) remained unchanged. For the adequate numerical evaluation of visual transformation it is necessary to ensure that calibration elements have the same brightness intensity on each couple of compared images. Rest of masked white regions (3x8) were extracted for following dominant color evaluation.

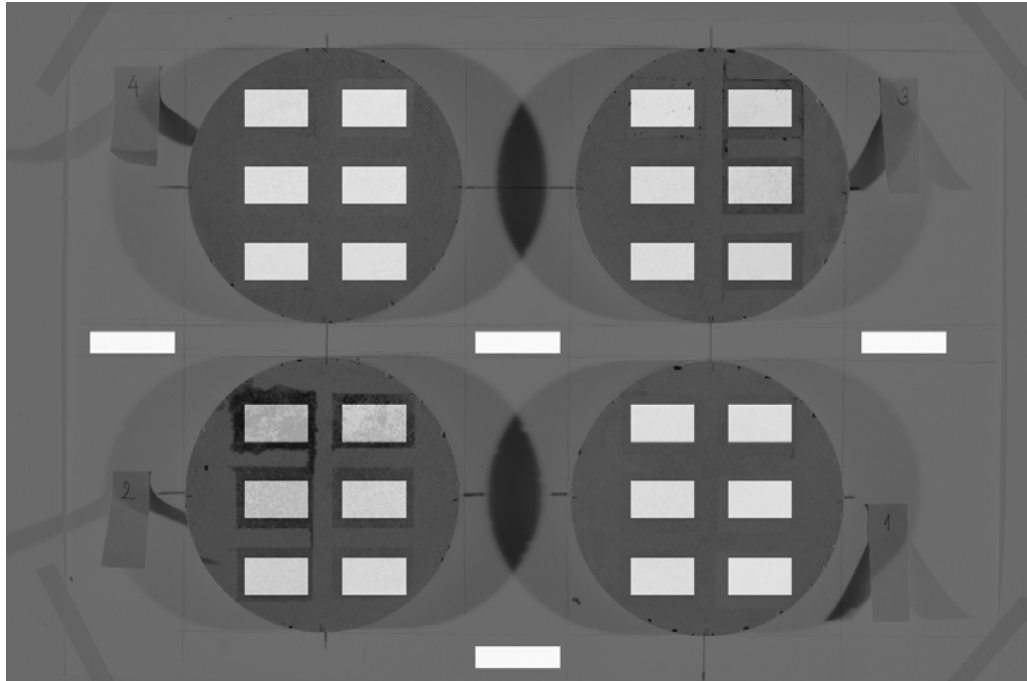


Fig. 24: Processing of the image data in Matlab - check of the fields' positions

4.5.2 Results interpretation

The output of the code is the palette – colorful pattern composed of 46 fields. The image may serve as infographics for presentation of the color change when description is added. There are 3 columns as number of different durations and 8 rows as number of substances. There is found a doubled field, which displays a fragment of the surface “before” the damage and same fragment “after” at the row/column intersection.

	5 sec	5 min	5 hours
Cleffect			
Water			
Dark liqueur			
Coffee			
Pumpkinseed oil			
Hand cream			
Soy sauce			
Vinegar			

Fig. 25: Reading the output pattern obtained through Matlab processing

Matlab code also composes matrices filled with numerical designation for the fields. Another output is a table. To each doubled fields there are four assigned values R,G,B and I identifying change in dominant tone. Positive value identifies lightening of the tone, negative – darkening. Absolute values of the differences (tone shifts) are summarizes to evaluate overall visual changeability of studied surface.

Number of the table on the right-hand side are adjusted by the “correction value”, which is computed based on error of “calibration elements”. The mismatch of the background is not constant along the image. It is -2 on the left edge of a photo and -1 on the right in the case displayed. General recommendation is to use for the input such images that would give the “correction value” as small as possible, in other words those which requires least correction. This difference seems to be negligible although calculating cumulative changeability may cause inaccuracy in a result.

Based on data of five tables (like in Fig. 26) it is useful to illustrate how change progresses in time (see Fig. 27). Analyzing this graph almost no difference can be found between unimproved U-sample and improved M+IM-sample. There might be distortion in values due to a product that affects surfaces most. Suspicious is that U, M, IM and M+IM can be observed to have nearly same summation of color changes by all 8 substances after 5 seconds test. However, such wrong impression happens due to the damage by vinegar which results in extremely visible light stains on dark concrete. And this great change by the single agent disregards the contribution of less aggressive substances.

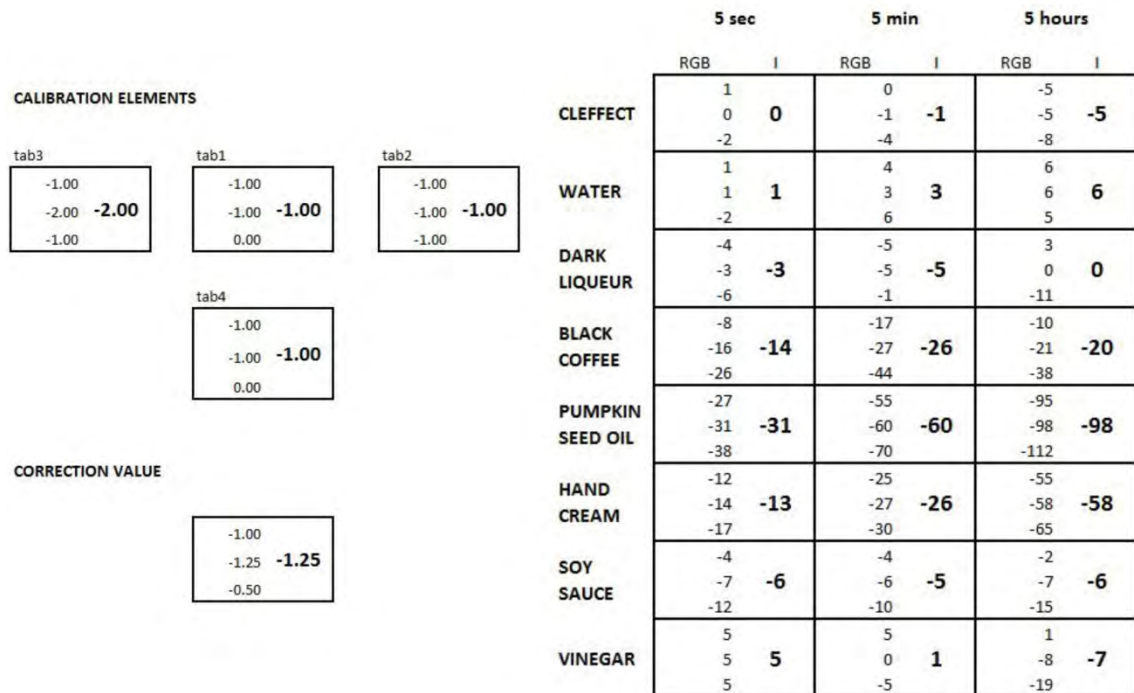


Fig. 26: Example of output of quantified visual transformation

It may be useful to separate the diagram into two (see Figs. 28 & 29) Used impregnation gives no effect in resisting to such acidic agent, therefore 5 second cumulative changes for U, M, IM and M+IM are in fact immediate change that vinegar made (Fig. 28). Color tone of the concrete plays an important role too: light gray UP-sample does not exhibit much of a visible change by vinegar.

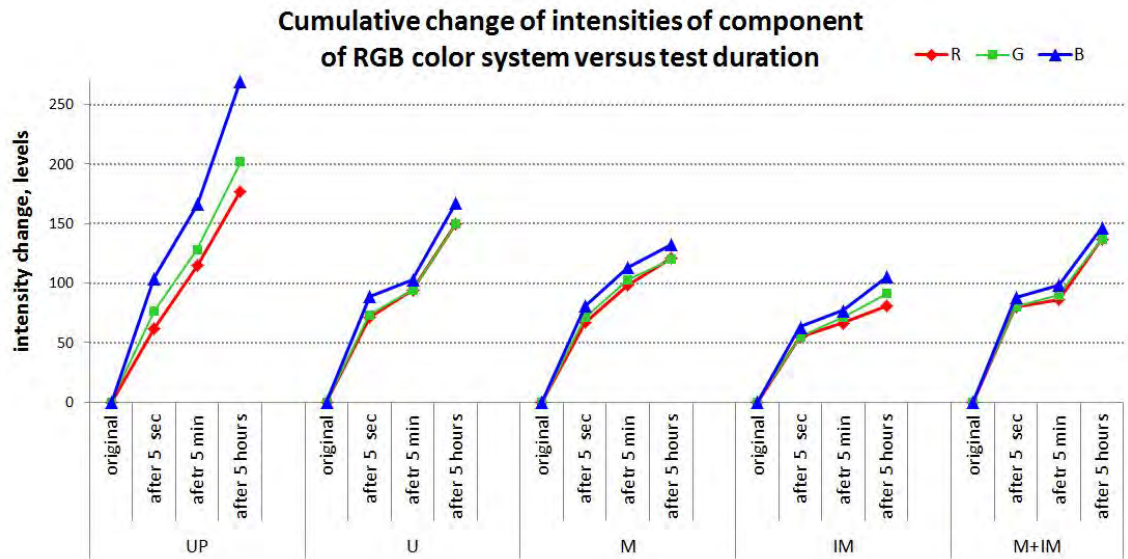


Fig. 27: Cumulative change of components' intensities of RGB color system - time dependent

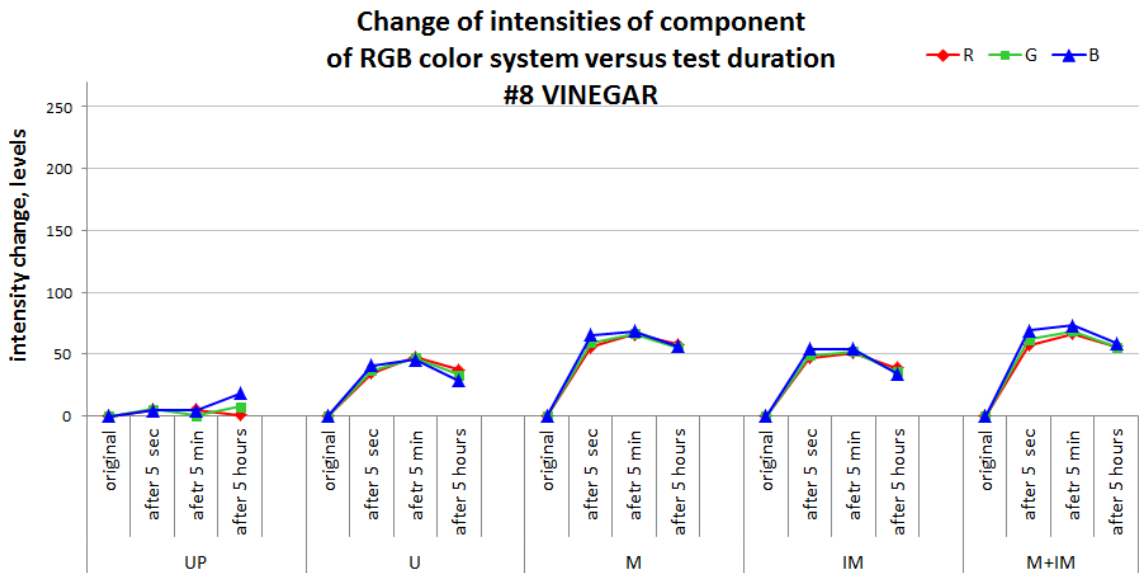


Fig. 28: Cumulative change of components' intensities of RGB color system - time dependent, after vinegar attack

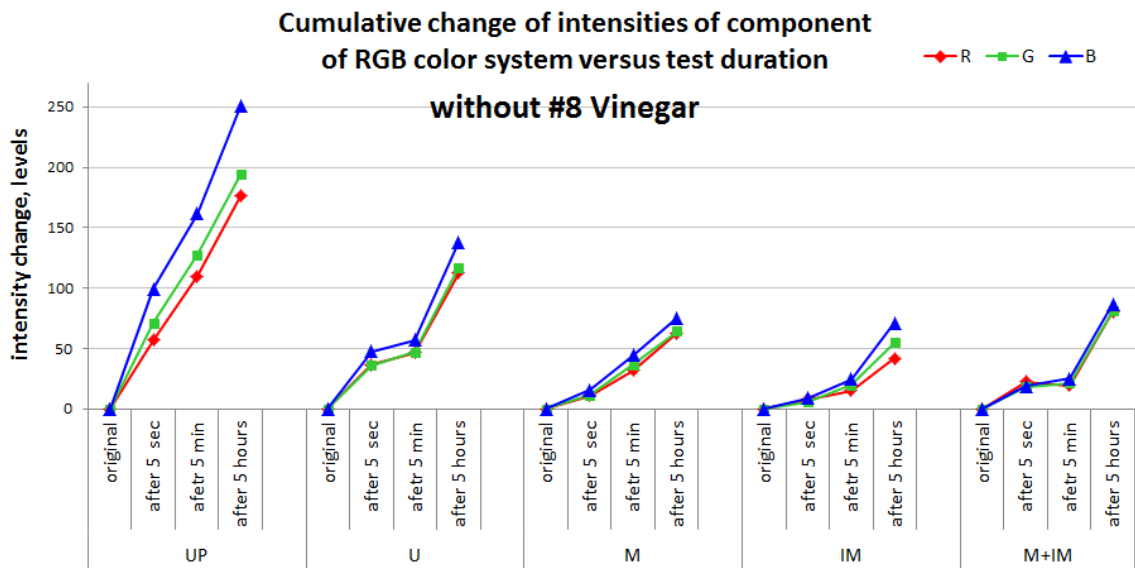


Fig. 29: Cumulative change of components' intensities of RGB color system - time dependent, vinegar attack excluded

This way (see Fig. 29) the effect of impregnation can be observed: IM and M+IM samples exhibit smaller damage to appearance after 5 minutes test than others surfaces. Character of lines are more alike to curves from the previous test of surface water uptake. Short test duration better reveals difference between surfaces whilst longer test duration reveals analogous resistance to chemical damage.

The surprising result is the ending of the curve of M+IM sample. Controversy to expectations surfaces M and IM appeared to be more resistant to substances #5 (Pumpkin seed oil) and #6 (Hand cream) separately than in its combination - M+IM treated sample. And since those product leads to evident discoloration and significantly contributes to overall summation of changes, M+IM sample does not display improvement in resistance according to gained data.

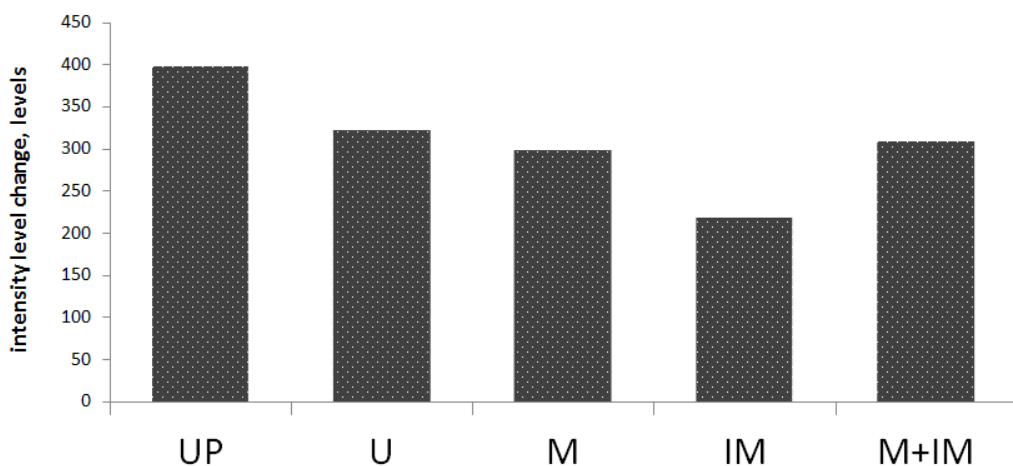


Fig. 30: Total cumulative change of Brightness Intensity Levels

Total summation (Fig. 30) gives an image about how surfaces maintain visual characteristic generally. From highest visible change to smallest the samples are: UP - 124%, U - 100%, IM+M - 93%, M - 67%, IM - 96% . This trend is also observed for all test durations in Fig. 29.

4.6 Abrasive wear test

Some of the applications of decorative concrete are associated with manipulation on its surface. Rubbing and scraping occurs due to cleaning, as well as falling or sliding of objects on the surface, therefore abrasion resistance becomes relevant for such application. In the scope of this test 3 sets of UP, U, M, IM, M+IM samples have been measured for comparison of their resistance to abrasive damage.

4.6.1 Experiment procedure

Handmade custom machine was constructed for that testing. Rotary engine brings in motion four weights (screws) hanging on light chains. The target (wooden frame) with the fixed sample is brought closer to the circular trajectory of the weights, the position is found where all weights stroke the surface, the target got fixed and that position is kept for the whole group to ensure that strokes are coming to the same place of the surface.

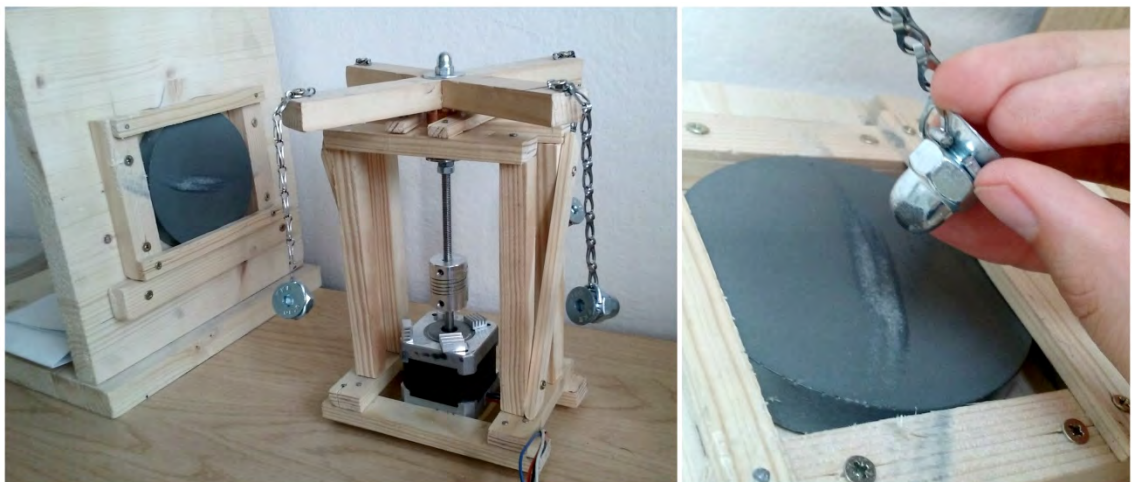


Fig. 31: Experimental setup - abrasion wear test

Matlab program was used for analysis of audio records with the sound of test in action. Blow forces are not same, that is well distinguished from Fig. 32. Some weights do the hitting action while other weights slide the surface, and there are also “skipped” strokes. This is due to oscillation of the axis of rotation during running of the engine, that vibration was not eliminated completely. Calculation of amplitude peaks allows evaluation of the total number of strokes within test cycle. 1 hour is equivalent to approximately 12000 hit by 8 g weight at the angle between 10 - 30 degrees with estimated velocity 1.25 m/s.

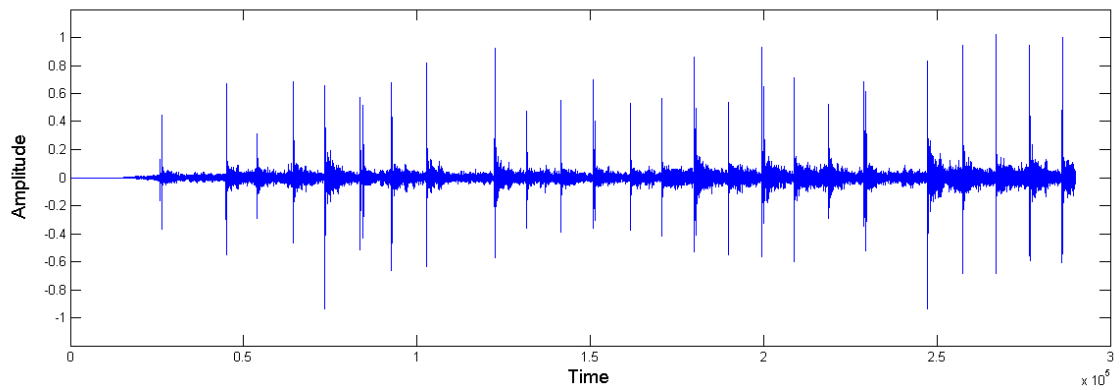


Fig. 32: Sound analysis performed in Matlab

All samples were exposed to abrasive damaging for 3 hours. Several measurements of the sample's weight were done throughout 3-hour testing. Cumulative wear loss displayed on the Fig. 33, separately for each of 3 groups which are distinguished by the change of worn region. The lines are outcome of 6 measurements throughout 3-hour time interval. It seems that wear loss is increasing linearly.

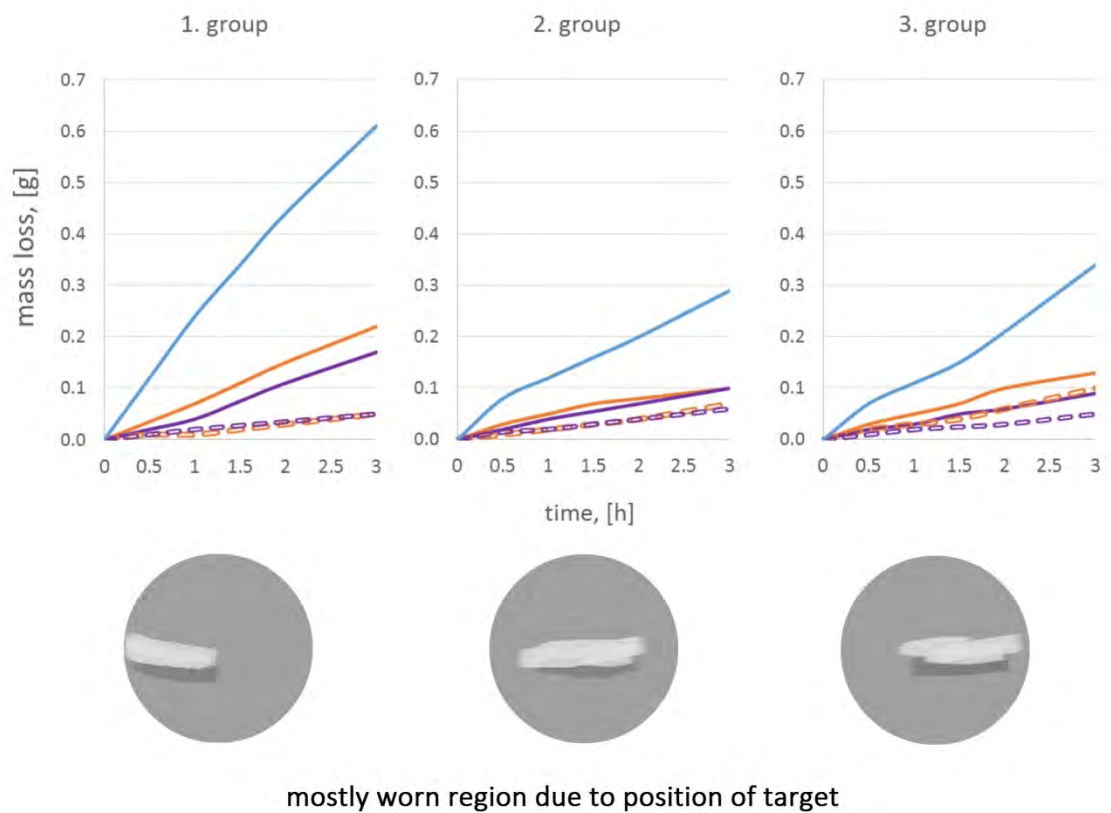


Fig. 33: Cumulative wear loss for different groups of samples

4.6.2 Results Interpretation

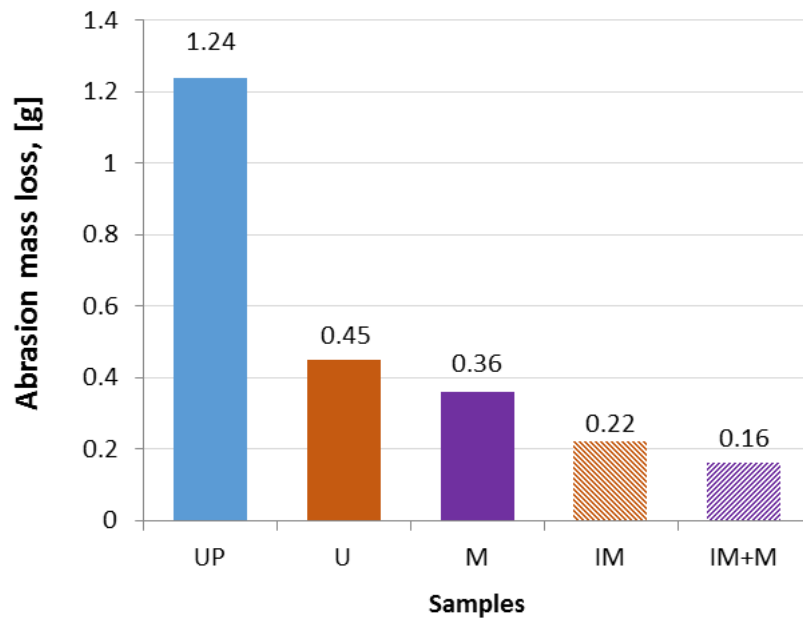


Fig. 34: Summation of abrasion loss of all 3 groups

Untreated Portland cement mortar resulted in about 2.7 time higher surface loss than untreated high strength mortar. Compared with untreated surface U improved samples M, IM and M+IM gave 20%, 51% and 65% smaller surface loss.

From the obtained data it is not clearly evident that the preparation of the surface before impregnation might have a positive effect of abrasive resistance. More evident is that application of impregnating product improves mechanical characteristics. This effect of surface restraining is also stated by the producer. It is also possible that reduction in surface permeability after impregnation led to “conservation” of water in IM and IM+M samples. Therefore less water escaped those surfaces, what allowed hydrating higher amount of cement. Sensitivity of mixes with low w/c ratio to water loss has been already mentioned in chapter 4.1.3. So there might be an improving in mechanical properties according to more favourable conditions provided to those samples in the following stages of hardening.

Other observation is slight weakening of the surface towards edges of the sample. Also higher value close to the edge (1.group) could happen due to spalling of small pieces from the edge, which could lead to this difference since measured quantities are very small.

5 SUMMARY

5.1 General conclusions

General conclusions can be drawn from the results obtained in this investigation:

1. Utilization of proposed **HSM mixture**

- led towards significant water penetration reduction, resulted in sorptivity value 1.41 kg/(m² s^{1/2}) of HSM with initial saturation of 73% mix versus 6.53 kg/(m² s^{1/2}) for PPCM with initial saturation of 35%
- reduced abrasion loss by 60%.
- resulted in much darker tone than PPCM, did contribute significantly to the resisting to visual degradation.

2. There is positive **effect of top hydrated cement removal** that has been done in M and M+IM samples:

- Constant 20% and 56% decrease in abrasion wear loss for non-impregnated samples and samples with impregnation respectively.
- It reduced surface absorption maximum by up to 54% for untreated surface (after 1.5 min of contact with water)
- It reduces surface absorption maximum by up to 66% for surfaces that has been impregnated and waxed (between 10 - 20 min of contact with water)
- Apparent improve can be distinguished only in short action of chemical agent, for example 5 minutes.
- Enhances effect of chemical hydrophobizing treatment. Postpones the beginning of water uptake from 2 min to 10 - 20 min

3. **Effectiveness of the water repellent nanoimpregnation and varnish** for IM and M+IM samples estimated as:

- 51% and 56% reduction in abrasion loss for original surface and for grinded surface respectively.
- Up to 70% decrease (achieved at 1.5 min) and up to 75% decrease (10 - 20 min) in amount of raised water for original glossy surface and for grinded surface respectively.
- Negligible except for short duration of chemical damage. No effect in resisting to an acidic solution such as vinegar.

4. In general, the positive effect for both mechanical and chemical treatments becomes less evident as liquid agent penetrates deeper into the surface. Since there is no barrier protection and the mortar matrix underlying top surface layer is the same for samples U, M, IM, M+IM the effect of treatments is time dependent (limited).
5. Prolongation of curing of visual surface in the airtight form leads to permanent darker shade. It was observed that the rate of color change immediately after unmoulding is higher when shorter duration of curing in airtight form applied.

5.2 Applicability

Mix design, proper selection of materials, design of practical mould and selection of an optimum treatment system are of great importance in widening the applicability range of a visual surface.

High workability of proposed mixture involves filling out forms with good detailing without vibration. On one hand the proposed mixture is 4 times more expensive. On the other hand actual consumption of impregnation depends on the surface roughness, the absorbency of the material and method of application; it is economically beneficial to apply it on smooth surface with refined pore structure. Explored surfaces are not recommended to exterior use as street and garden furniture or external façade claddings. The range of indoor applicability is summarized below:

Recommended treatment types	Exposure category	Examples of products
-	Severe in terms of exposure to household chemicals or prolonged contact with water	Tiles at cooking areas, kitchen countertops, bar counters, tableware, sink, washing basins, bathtub, water reservoirs, fountains
M+IM	Short period of exposure to aggressive agents	Dining table, kitchen paneling other countertops, trays, bowls, containers
IM, M, M+IM	Wet cleansing may be applied	Seating, stools, shelving, pots, vases lamp shade, cases, desktop accessories, jewelry, wearable body accessories
U, IM, M, M+IM	Does not require wet cleaning	Decorative tile, Sculpture, Interior cladding, Artwork

Tab. 13: Applicability of studied surface treatments

5.3 Future research recommendations

Production of a full-size sample is necessary to implement in order to test the feasibility of the formwork and to make final resolutions on visual appearance.

Quantify the durability based on the outcomes of the experimental analyses which were performed within the scope of this master thesis.

Estimate production costs and evaluate the cost efficiency of the technique.

Bibliography

- [1] Graphic relief. [online]. [cit. 2016-15-03] Available from: <http://graphicrelief.co.uk/gallery/>.
- [2] Jayson L Helsel. Some hard truths on concrete coatings and coverings. *Journal of Architectural Coatings*, 3(1):70–71, 2007.
- [3] Architectural finishes. [online]. [cit. 2016-18-03] Available from: http://www.wilcoprecast.co.nz/architectural_finishes.html.
- [4] Bernard Thomas Benn. *The influence of curing and surface preparation on the adhesion of protective coatings on concrete*. PhD thesis, 2010.
- [5] Robert W Gaul. Preparing concrete surfaces for coatings. *Concrete International*, 6(7):17–22, 1984.
- [6] Concrete surface preparation. [online]. [cit. 2016-01-04] Available from: <http://blastjournal.com/concrete-surface-preparation-a-primer-3/>.
- [7] Düramen. [online]. [cit. 2016-10-05] Available from: <http://www.duraamen.com/blog/concord-new-hampshire-epoxy-repair/#.V0raKpF96M..>
- [8] Troubleshooting 5 common sealer problems. [online]. [cit. 2016-30-04] Available from: <http://www.forconstructionpros.com/article/10281592/how-to-prevent-decorative-concrete-sealer-problems>.
- [9] SP Zhang and L Zong. Evaluation of relationship between water absorption and durability of concrete materials. *Advances in Materials Science and Engineering*, 2014, 2014.
- [10] MJ Shannag. High strength concrete containing natural pozzolan and silica fume. *Cement and Concrete Composites*, 22(6):399–406, 2000.
- [11] Rafat Siddique and El-Hadj Kadri. Effect of metakaolin and foundry sand on the near surface characteristics of concrete. *Construction and Building Materials*, 25(8):3257–3266, 2011.
- [12] Jeenu G. Vinod P., Lalu Mangal. Durability studies on high strength high performance concrete. *International journal of civil engineering and technology*, 4(1):16–25, January - February 2013.
- [13] A Dubosc, G Escadeillas, and PJ Blanc. Characterization of biological stains on external concrete walls and influence of concrete as underlying material. *Cement and Concrete Research*, 31(11):1613–1617, 2001.

- [14] Fu Tung Cheng. *Concrete countertops: Design, forms, and finishes for the new kitchen and bath*. Taunton Press, 2004.
- [15] Acid attack on concrete. [online]. [cit. 2016-19-03] Available from: <http://www.concrete-experts.com/pages/acid.htm>.
- [16] EN DIN. 206-1: Beton. *Festlegung, Eigenschaften, Herstellung und Konformität*, 2001.
- [17] DM Roy, P Arjunan, and MR Silsbee. Effect of silica fume, metakaolin, and low-calcium fly ash on chemical resistance of concrete. *Cement and Concrete Research*, 31(12):1809–1813, 2001.
- [18] Esam Elawady, Amr A El Hefnawy, and Rania AF Ibrahim. Comparative study on strength, permeability and sorptivity of concrete and their relation with concrete durability. *International Journal of Engineering and Innovative Technology (IJEIT)*, 4, 2014.
- [19] Andreas Koenig and Frank Dehn. Main considerations for the determination and evaluation of the acid resistance of cementitious materials. *Materials and Structures*, pages 1–11, 2015.
- [20] Edward G Nawy. *Concrete construction engineering handbook*. CRC press, 2008.
- [21] Alan B Poole and Ian Sims. *Concrete petrography: a handbook of investigative techniques*. Arnold; Copublished in North, Central and South America by J. Wiley, second edition, 2015.
- [22] Albertas Klovas and Mindaugas DAUKŠYS. The evaluation methods of decorative concrete horizontal surfaces quality. *Materials Science*, 19(3):343–348, 2013.
- [23] Pavel Reiterman. Vliv technologie na vlastnosti povrchových vrstev pohledového betonu. 2013.
- [24] Your guide to using bayferrox pigments to color concrete products. [online], 2004. [cit. 2016-08-05] Available from: http://bayferrox.com/uploads/tx_lxsmatrix/Guide_to_Pigmenting_Concrete_02.pdf.
- [25] Elkem. *User Guide, Elkem Materials Mixture Analyser – EMMA*. [cit. 2016-11-04] Available from: <https://www.elkem.com/documents/software/emma-user-doc.pdf>.
- [26] Randall M German. Particle packing characteristics. 1989.
- [27] Michael Haase. *Kontrola kvality při výrobě cementu*. 2012.
- [28] Mario Collepari. *Moderní beton*. Pro Českou komoru autorizovaných inženýrů a techniků činných ve výstavbě (ČKAIT) vydalo Informační centrum ČKAIT, 2009.
- [29] Sofia Utsi. Performance based concrete mix-design: aggregate and micro mortar optimization applied on self-compacting concrete containing fly ash. 2008.

- [30] Michael Schmidt, Ekkehard Fehling, Christoph Glotzbach, Susanne Fröhlich, and Siemon Piotrowski. Ultra-high performance concrete and nanotechnology in construction. *Proceedings of Hipermat*, pages 7–9, 2012.
- [31] Self-consolidating concrete, visual stability index (vsi). [online]. [cit. 2016-15-04] Available from: <https://assets.master-builders-solutions.basf.com/Shared>
- [32] Concrete surfaces – beautiful solutions with aalborg white. [online]. [cit. 2016-25-04] Available from: http://www.aalborgwhite.com/media/pdf_files/info_concrete_surfaces.pdf.
- [33] Canan Tasdemir. Combined effects of mineral admixtures and curing conditions on the sorptivity coefficient of concrete. *Cement and Concrete Research*, 33(10):1637–1642, 2003.
- [34] Geert De Schutter and Katrien Audenaert. *Report 38: Durability of Self-Compacting Concrete-State-of-the-Art Report of RILEM Technical Committee 205-DSC*, volume 38. RILEM publications, 2007.
- [35] Nicos S Martys and Chiara F Ferraris. Capillary transport in mortars and concrete. *Cement and Concrete Research*, 27(5):747–760, 1997.
- [36] AM Neville. Properties of concrete, trans, 2011.
- [37] R Nokken Michelle and Douglas Hooton. Dependence of rate of absorption on degree of saturation of concrete. *Cement, concrete and aggregates*, 24(1):20–24, 2002.
- [38] H Abdul Razak, HK Chai, and HS Wong. Near surface characteristics of concrete containing supplementary cementing materials. *Cement and concrete composites*, 26(7):883–889, 2004.
- [39] Eva Vejmelkova, Milena Pavlikova, Martin Keppert, Zbyněk Keršner, Pavla Rovnaníková, Michal Ondráček, Martin Sedlmajer, and Robert Černý. High performance concrete with czech metakaolin: Experimental analysis of strength, toughness and durability characteristics. *Construction and Building Materials*, 24(8):1404–1411, 2010.
- [40] Kazim Turk and Mehmet Karatas. Abrasion resistance and mechanical properties of self-compacting concrete with different dosages of fly ash/silica fume. *Indian Journal of Engineering & Materials Sciences*, 18(1):49–60, 2011.

List of Figures

1	Black web, pattern by Sarah Arnett. White concrete. Adopted from [1] . . .	4
2	10 grades of surface of roughness for different treatment types	6
3	From left to right: epoxy coating failure [7], blushing and bond failure, bubbles in a sealer [8]	7
4	Impact of uneven drying	12
5	Surface discoloration	13
6	Sample of the image data	13
7	Illustration of mean, median and mode values	15
8	Typical histogram of a light color shade	15
9	Typical histogram of a dark color shade	16
10	Intensity levels on grayscale 0-255 measured on 38 th day for surfaces with different duration of treatment	17
11	Color transition throughout time	17
12	Brightness transition for surfaces #1 - #6 with assigned values	18
13	Particle size distribution curve of proposed HSM	23
14	Mini slump testing of HSM and PPCM	26
15	Petri dish	27
16	Visual appearance of M (left) & U (right) treatments	28
17	Arrangement of the surface water absorption test	30
18	Vertical water uptake - 3 hours	32
19	Vertical water uptake - 10 minutes	32
20	Trendlines of vertical water uptake	33
21	Arrangement of chemical attack test	37
22	Application of tested substances onto surface samples	37
23	Photo studio setup for collection of image data	38
24	Processing of the image data in Matlab - check of the fields' positions . . .	39
25	Reading the output pattern obtained through Matlab processing	39
26	Example of output of quantified visual transformation	40
27	Cumulative change of components' intensities of RGB color system - time dependent	41
28	Cumulative change of components' intensities of RGB color system - time dependent, after vinegar attack	41
29	Cumulative change of components' intensities of RGB color system - time dependent, vinegar attack excluded	42
30	Total cumulative change of Brightness Intensity Levels	42

31	Experimental setup - abrasion wear test	43
32	Sound analysis performed in Matlab	44
33	Cumulative wear loss for different groups of samples	44
34	Summation of abrasion loss of all 3 groups	45
35	Color transformation of the UP-sample	69
36	Color transformation of the U-sample	70
37	Color transformation of the M-sample	71
38	Color transformation of the IM-sample	72
39	Color transformation of the M+IM-sample	73

List of Tables

1	Exposure classes for chemical attack according to DIN EN 206-1 [16]	9
2	Chronology of data collection for experimental study of effect of curing duration on a final color of concrete	14
3	Particle size distribution for selected constituents	21
4	High strength mortar mix recipe	22
5	Plain Portland cement mortar mix recipe	23
6	Mixing procedure	24
7	Basic physical characteristics of studied mixtures	25
8	Notations of the categories of samples according to applied treatment	27
9	Schedule of experimental part	29
10	Sorptivity values obtained from water uptake trendlines	34
11	Characteristics of mixtures with high share of SCMs	35
12	Substances used in chemical attack testing	36
13	Applicability of studied surface treatments	47

Appendices

A Matlab Syntax

```
clc;
clear all variables;
clear all;
close all;
```

Input of the photos

```
Ipo=imread('C:\Users\Nadi\Desktop\JPEG po\1.2.jpg');
Ipred=imread('C:\Users\Nadi\Desktop\JPEG pred\1.jpg');

% Get the dimensions of the image
[rows, columns, numberOfColorBands] = size(Ipo);
```

Initialize parameters for the rectangular fields, it's location, sizes and spacing

```
height = 140; halfheight = height/2;
width = 240; halfwidth = width/2;

hs = 370;           % horizontal spacing between stains
hb = 1460;          % horizontal spacing between samples
vs = 290;           % vertical spacing between stains
vb = 1190;          % vertical spacing between samples

CenX=1030; CenY=410;

% position of the left upper surface
CenX1 =CenX;        CenX4 =CenX+hs;
CenY1 =CenY;        CenY4 =CenY;

CenX2 =CenX;        CenX5 =CenX+hs;
CenY2 =CenY+vs;    CenY5 =CenY+vs;

CenX3 =CenX;        CenX6 =CenX+hs;
CenY3 =CenY+vs*2;  CenY6 =CenY+vs*2;

% position of the right upper surface
CenX7 =CenX+hb;    CenX10 =CenX+hb+hs;
CenY7 =CenY;       CenY10 =CenY;

CenX8 =CenX+hb;    CenX11 =CenX+hb+hs;
CenY8 =CenY+vs;    CenY11 =CenY+vs;
```

```

CenX9 =CenX+hb;   CenX12 =CenX+hb+hs;
CenY9 =CenY+vs*2; CenY12 =CenY+vs*2;

% position of the left bottom surface
CenX13 =CenX;     CenX16 =CenX+hs;
CenY13 =CenY+vb;  CenY16 =CenY+vb;

CenX14 =CenX;     CenX17 =CenX+hs;
CenY14 =CenY+vs+vb; CenY17 =CenY+vs+vb;

CenX15 =CenX;     CenX18 =CenX+hs;
CenY15 =CenY+vs*2+vb; CenY18 =CenY+vs*2+vb;

% position of the right bottom surface
CenX19 =CenX+hb;   CenX22 =CenX+hb+hs;
CenY19 =CenY+vb;   CenY22 =CenY+vb;

CenX20 =CenX+hb;   CenX23 =CenX+hb+hs;
CenY20 =CenY+vs+vb; CenY23 =CenY+vs+vb;

CenX21 =CenX+hb;   CenX24 =CenX+hb+hs;
CenY21 =CenY+vs*2+vb; CenY24 =CenY+vs*2+vb;

% position of calibration fragments of background

CenXCalib2 = columns/2;   CenXCalib = columns/2;
CenYCalib2 = rows/2+vb;   CenYCalib = rows/2;

CenXCalib3 = columns/2-hb; CenXCalib4 = columns/2+hb;
CenYCalib3 = rows/2;     CenYCalib4 = rows/2;

```

Create vectors to contain all position coordinates

```

CenX=zeros(1,24);
CenY=zeros(1,24);
for i=1:24
    CenX(i)= eval(sprintf('CenX%d', i))-width/2;
    CenY(i)= eval(sprintf('CenY%d', i))-height/2;
end

```

Initialize an image to a logical image of rectangles

```

squareImage = false(rows, columns);
[x, y] = meshgrid(1:columns, 1:rows);

% Initialize calibration fields
squareImage(abs(x - CenXCalib)≤ 160 & abs(y - CenYCalib) ≤ 40) = true;
squareImage(abs(x - CenXCalib2)≤ 160 & abs(y - CenYCalib2) ≤ 40) = true;
squareImage(abs(x - CenXCalib3)≤ 160 & abs(y - CenYCalib3) ≤ 40) = true;

```

```

squareImage(abs(x - CenXCalib4) ≤ 160 & abs(y - CenYCalib4) ≤ 40) = true;
% Upper 12 fields
squareImage(abs(x - CenX1) ≤ halfwidth & abs(y - CenY1) ≤ halfheight) = true;
squareImage(abs(x - CenX2) ≤ halfwidth & abs(y - CenY2) ≤ halfheight) = true;
squareImage(abs(x - CenX3) ≤ halfwidth & abs(y - CenY3) ≤ halfheight) = true;
squareImage(abs(x - CenX4) ≤ halfwidth & abs(y - CenY4) ≤ halfheight) = true;
squareImage(abs(x - CenX5) ≤ halfwidth & abs(y - CenY5) ≤ halfheight) = true;
squareImage(abs(x - CenX6) ≤ halfwidth & abs(y - CenY6) ≤ halfheight) = true;
squareImage(abs(x - CenX7) ≤ halfwidth & abs(y - CenY7) ≤ halfheight) = true;
squareImage(abs(x - CenX8) ≤ halfwidth & abs(y - CenY8) ≤ halfheight) = true;
squareImage(abs(x - CenX9) ≤ halfwidth & abs(y - CenY9) ≤ halfheight) = true;
squareImage(abs(x - CenX10) ≤ halfwidth & abs(y - CenY10) ≤ halfheight) = ...
    true;
squareImage(abs(x - CenX11) ≤ halfwidth & abs(y - CenY11) ≤ halfheight) = ...
    true;
squareImage(abs(x - CenX12) ≤ halfwidth & abs(y - CenY12) ≤ halfheight) = ...
    true;
% Lower 12 fields
squareImage(abs(x - CenX13) ≤ halfwidth & abs(y - CenY13) ≤ halfheight) = ...
    true;
squareImage(abs(x - CenX14) ≤ halfwidth & abs(y - CenY14) ≤ halfheight) = ...
    true;
squareImage(abs(x - CenX15) ≤ halfwidth & abs(y - CenY15) ≤ halfheight) = ...
    true;
squareImage(abs(x - CenX16) ≤ halfwidth & abs(y - CenY16) ≤ halfheight) = ...
    true;
squareImage(abs(x - CenX17) ≤ halfwidth & abs(y - CenY17) ≤ halfheight) = ...
    true;
squareImage(abs(x - CenX18) ≤ halfwidth & abs(y - CenY18) ≤ halfheight) = ...
    true;
squareImage(abs(x - CenX19) ≤ halfwidth & abs(y - CenY19) ≤ halfheight) = ...
    true;
squareImage(abs(x - CenX20) ≤ halfwidth & abs(y - CenY20) ≤ halfheight) = ...
    true;
squareImage(abs(x - CenX21) ≤ halfwidth & abs(y - CenY21) ≤ halfheight) = ...
    true;
squareImage(abs(x - CenX22) ≤ halfwidth & abs(y - CenY22) ≤ halfheight) = ...
    true;
squareImage(abs(x - CenX23) ≤ halfwidth & abs(y - CenY23) ≤ halfheight) = ...
    true;
squareImage(abs(x - CenX24) ≤ halfwidth & abs(y - CenY24) ≤ halfheight) = ...
    true;

```

Preview - check the position of the field - fitting inside stain

```

Ipogray=rgb2gray(Ipo); Ipredgray=rgb2gray(Ipred);
II = im2double(Ipogray); AA = im2double(Ipredgray);

SquaresI = im2double(squareImage);
figure, imshow(SquaresI+II, []);
figure, imshow(SquaresI+AA, []);

```

```
drawnow;
```

Mask the image with the logical image for the preview of a pair of images

```
maskedImageIpo = bsxfun(@times, Ipo, cast(squareImage,class(Ipo)));  
  
maskedImageIpred = bsxfun(@times, Ipred, cast(squareImage,class(Ipred)));  
  
figure(), imshowpair (maskedImageIpo,maskedImageIpred, 'montage');
```

Getting histogram of the palette calibration element and writing element into file

```
temp = uint8(0);  
  
calibElementPo1(50,190,3)=temp;   calibElementPred1(50,190,3)=temp;  
calibElementPo2(50,190,3)=temp;   calibElementPred2(50,190,3)=temp;  
calibElementPo3(50,190,3)=temp;   calibElementPred3(50,190,3)=temp;  
calibElementPo4(50,190,3)=temp;   calibElementPred4(50,190,3)=temp;  
  
for i=1:50  
for j=1:190  
    calibElementPo1(i,j,:)=Ipo(i+CenYCalib-25-1,j+CenXCalib-95-1,:);  
    calibElementPred1(i,j,:)=Ipred(i+CenYCalib-25-1,j+CenXCalib-95-1,:);  
    calibElementPo2(i,j,:)=Ipo(i+CenYCalib2-25-1,j+CenXCalib2-95-1,:);  
    calibElementPred2(i,j,:)=Ipred(i+CenYCalib2-25-1,j+CenXCalib2-95-1,:);  
    calibElementPo3(i,j,:)=Ipo(i+CenYCalib3-25-1,j+CenXCalib3-95-1,:);  
    calibElementPred3(i,j,:)=Ipred(i+CenYCalib3-25-1,j+CenXCalib3-95-1,:);  
    calibElementPo4(i,j,:)=Ipo(i+CenYCalib4-25-1,j+CenXCalib4-95-1,:);  
    calibElementPred4(i,j,:)=Ipred(i+CenYCalib4-25-1,j+CenXCalib4-95-1,:);  
end;  
end;
```

Checking of matching of the background

```
% Reshaping images into vector of pixels values  
  
calibElementPredVector1 = reshape(calibElementPred1,50*190,1,3);  
calibElementPoVector1 = reshape(calibElementPo1,50*190,1,3);  
calibElementPredVector2 = reshape(calibElementPred2,50*190,1,3);  
calibElementPoVector2 = reshape(calibElementPo2,50*190,1,3);  
calibElementPredVector3 = reshape(calibElementPred3,50*190,1,3);  
calibElementPoVector3 = reshape(calibElementPo3,50*190,1,3);  
calibElementPredVector4 = reshape(calibElementPred4,50*190,1,3);  
calibElementPoVector4 = reshape(calibElementPo4,50*190,1,3);  
  
% Evaluate mismatching for the 1st calibration element
```



```

R=median(double(calibElementPredVector1(:,1)))-median(double(...
    calibElementPoVector1(:,1)));
G=median(double(calibElementPredVector1(:,2)))-median(double(...
    calibElementPoVector1(:,2)));
B=median(double(calibElementPredVector1(:,3)))-median(double(...
    calibElementPoVector1(:,3)));
I=median(double(reshape(rgb2gray(calibElementPred1),50*190,1)))-median(...
    double(reshape(rgb2gray(calibElementPo1),50*190,1)));

RGB_CHANGE_CALIBRATION_median(1,:)= [R,G,B,I];

% Evaluate mismatching for the 2nd calibration element

R=median(double(calibElementPredVector2(:,1)))-median(double(...
    calibElementPoVector2(:,1)));
G=median(double(calibElementPredVector2(:,2)))-median(double(...
    calibElementPoVector2(:,2)));
B=median(double(calibElementPredVector2(:,3)))-median(double(...
    calibElementPoVector2(:,3)));
I=median(double(reshape(rgb2gray(calibElementPred2),50*190,1)))-median(...
    double(reshape(rgb2gray(calibElementPo2),50*190,1)));

RGB_CHANGE_CALIBRATION_median(2,:)= [R,G,B,I];

% Evaluate mismatching for the 3rd calibration element

R=median(double(calibElementPredVector3(:,1)))-median(double(...
    calibElementPoVector3(:,1)));
G=median(double(calibElementPredVector3(:,2)))-median(double(...
    calibElementPoVector3(:,2)));
B=median(double(calibElementPredVector3(:,3)))-median(double(...
    calibElementPoVector3(:,3)));
I=median(double(reshape(rgb2gray(calibElementPred3),50*190,1)))-median(...
    double(reshape(rgb2gray(calibElementPo3),50*190,1)));

RGB_CHANGE_CALIBRATION_median(3,:)= [R,G,B,I];

% Evaluate mismatching for the 4th calibration element

R=median(double(calibElementPredVector4(:,1)))-median(double(...
    calibElementPoVector4(:,1)));
G=median(double(calibElementPredVector4(:,2)))-median(double(...
    calibElementPoVector4(:,2)));
B=median(double(calibElementPredVector4(:,3)))-median(double(...
    calibElementPoVector4(:,3)));
I=median(double(reshape(rgb2gray(calibElementPred4),50*190,1)))-median(...
    double(reshape(rgb2gray(calibElementPo4),50*190,1)));

RGB_CHANGE_CALIBRATION_median(4,:)= [R,G,B,I];

```

Displaying matrix of the variance in tone and brightness levels

```
disp( RGB_CHANGE_CALIBRATION_median );
```

Specifying the correction values

```
correction_Red= median( RGB_CHANGE_CALIBRATION_median(:,1) )  
correction_Green= median( RGB_CHANGE_CALIBRATION_median(:,2) )  
correction_Blue= median( RGB_CHANGE_CALIBRATION_median(:,3) )
```

Calibration of the input images

```
Ipred(:, :, 1)=Ipred(:, :, 1)-uint8( correction_Red );  
Ipred(:, :, 2)=Ipred(:, :, 2)-uint8( correction_Green );  
Ipred(:, :, 3)=Ipred(:, :, 3)-uint8( correction_Blue );
```

Output pattern compilation

```
for line=1:8  
    fprintf(' LINE %i\n',line)  
    s=0;  
    for window=line*3:-1:line*3-2  
        fprintf(' COUPLE NUMBER %i\n',window)  
        Pred(height,width,3)=temp;  
        Po(height,width,3)=temp;  
        for x=1:height  
            for y=1:width  
                Pred(x,y,:)=Ipred(x+CenY(window)-1,y+CenX(window)-1,:);  
                Po(x,y,:)=Ipo(x+CenY(window)-1,y+CenX(window)-1,:);  
            end  
        end  
        PredGray = rgb2gray(Pred);  
        PoGray = rgb2gray(Po);  
        PredVector = reshape(Pred,height*width,1,3);  
        PoVector = reshape(Po,height*width,1,3);  
  
        % Filling in the matrix of the color transition for particular couple of ...  
        fields  
        R=median(double(PredVector(:,1)))-median(double(PoVector(:,1)));  
        G=median(double(PredVector(:,2)))-median(double(PoVector(:,2)));  
        B=median(double(PredVector(:,3)))-median(double(PoVector(:,3)));  
        I=median(double(reshape(PredGray,height*width,1))-median(double(...  
            reshape(PoGray,height*width,1)));  
  
        RGB_CHANGE_MEDIAN(window,:)= [R,G,B,I];  
  
        % Generate a doublefield "before" and "after"  
        Couple(height,width*2,3)=temp;  
        for x=1:height  
            for y=1:width
```

```

        Couple(x,y,:)=Pred(x,y,:);
        Couple(x,y+width,:)=Po(x,y,:);
    end
end

% Generate a line of three doubled fields
Line(height,width*6,3)=temp;
for x=1:height
    for y=1:width*2
        Line(x,y+width*2*s,:)=Couple(x,y,:);
    end
end
s=s+1;
end;

% Generate a block of 12 lines
Block(height*8,width*2,3)=temp;
for x=1:height
for y=1:width*6
Block(x+height*(line-1),y,:)=Line(x,y,:);
end
end
end

    figure(), imshow(Block);
    disp( RGB_CHANGE_MEDIAN );

% Saving the generated pattern
imwrite(Block,'C:\Users\Nadi\Desktop\Chemical damage\PPCM.png');

```



Mletý vápenec D8

List : CaCO₃ D8
Označení : IOD.LAB.04

Datum : 21.01.2008
LV č. 4

Popis produktu

Přírodní surovina - mletý vápenec druh 8 podle ČSN 721220

Možnosti použití

- chemický průmysl
- sklářský průmysl
- keramický průmysl
- zdravotnický průmysl

CHEMICKÉ SLOŽENÍ

(ve shodě se standardními analytickými metodami)

	min. (%)	max. (%)	charakteristické rozpětí (%)
CaCO ₃	95,5		99 – 99,4
MgCO ₃		2,0	0,7 – 1
Fe ₂ O ₃		0,06	0,035 – 0,045
Al ₂ O ₃		0,4	0,035 – 0,055
SiO ₂		1,5	0,04 – 0,14
MnO		0,03	0,003 – 0,007
SO ₃		0,1	0,02 – 0,06

GRANULOMETRIE

Granulometrie	min. (%)	max. (%)	charakteristické rozpětí (%)
> 0,09 mm		20	15 - 19
> 0,50 mm		0,2	

FYZIKÁLNÍ VLASTNOSTI

	charakteristické rozpětí (%)
Sypná hmotnost (kg/dm ³)	0,99 – 1,08

Dodávky

- volně ložený materiál v silokamionech a silovagónech
- materiál v big bagu (1000 kg, 500 kg)
- materiál pytlovaný (25 kg, 1000 kg na paletě)

Uskladnění

- chraňte před vlhkostí

Bezpečnost

- bezpečnostní list (www.lhoist.cz)

TECHNICKÉ PÍSKY

Písky s extrémně vysokým obsahem SiO_2 jsou vynikající surovinou ve vodárenství k filtrování pitné vody a technologických vod, pro nejrůznější použití ve strojírenství, pro technologii přesného lití, ve stavebnictví jako plnivo do průmyslových podlah, na tryskání betonových a ocelových konstrukcí, na zásyp umělých sportovních trávníků apod. Technický písek s malým obsahem Fe_2O_3 je vynikající surovinou v elektrotechnickém průmyslu jako hasivo do pojistek vysokého napětí, jako zásypová a izolační hmota v elektrických topných tělesech a v dalších oborech.

Písky se dodávají sušené, volně ložené a balené, pro nakládku na silniční nebo železniční dopravní prostředky.

ZRNITOSTNÍ DATA A VLASTNOSTI TÝKAJÍCÍ SE VELIKOSTI ČÁSTIC

	ST 01/06	ST 02/06	ST 03/08	ST 06/12	STF 06/12	ST 10/40	Metody
Velikost středního zrna (d50)	0,36	0,35	0,55	0,93	0,91	1,98	mm sítování
AFS	33	32	23	15	15	5	sítování
sypaná hmotnost	1,52	1,5	1,5	1,52	1,52	1,55	kg/l
> 4000 μm				3,6	3	0	% sítování
> 1250 μm	0	0	0			99	% sítování
> 1000 μm			5,2				% sítování
> 800 μm	7,9	0,17		94,2	96,6		% sítování
> 630 μm							% sítování
> 500 μm			93,5			1	%
> 315 μm	86,5	98,33					% sítování
> 200 μm				2,2			% sítování
> 100 μm	5,4	1,5	1,3		0,4		% sítování
< 100 μm	0,2						% sítování

CHEMICKÉ ANALÝZY (RFA) %

	ST 01/06	ST 02/06	ST 03/08	ST 06/12	STF 06/12	ST 10/40
SiO_2	99,2	99,4	99,4	99,2	99,3	99,2
Fe_2O_3	0,04	0,02	0,02	0,03	0,03	0,03

FYZIKÁLNÍ CHARAKTERISTIKA

hustota (g/ml)	2,65	vlhkost (%)	0,2 max
tvrdost, Mohs	7	pH	7,2
ztráta žíháním (%)	0,1 - 0,3		

Křemenný písek ze Střelče je upravená přírodní surovina. Výše uvedené informace jsou založeny na středních hodnotách. Data by měla být považována pouze za indikativní. Hrubší a jemnější podíly jsou ve stopových množstvích možné. Uživateli přísluší, aby nejprve otestoval a posoudil vhodnost použití pro svůj účel. O případných tolerancích výše uvedených hodnot výrobků je možné jednat.

Prodej a dodávání je vždy na základě sjednaných obchodních podmínek a podle příslušné podnikové normy nebo kvalitativní dohody.

Datum revize: 1.5.2016

CEM I 42,5 R

Portlandský cement

EN 197-1

Výrobní závod: **Mokrá**
 Výrobce: **Českomoravský cement, a.s.**

Technický list

Vlastnost	Průměrná hodnota	Jednotka	Metoda / poznámka
Mechanické vlastnosti			
pevnost v tlaku	1 den	17	[MPa] EN 196-1
	2 dny	29	[MPa] EN 196-1
	7 dní	51	[MPa] EN 196-1
	28 dní	61	[MPa] EN 196-1
	56 dní	66	[MPa] EN 196-1
	90 dní	67	[MPa] EN 196-1
pevnost v tahu za ohybu	1 den	4	[MPa] EN 196-1
	2 dny	6	[MPa] EN 196-1
	7 dní	8	[MPa] EN 196-1
	28 dní	9	[MPa] EN 196-1
	56 dní	9	[MPa] EN 196-1
	90 dní	9	[MPa] EN 196-1
Fyzikální vlastnosti			
normální konzistence	28,0	[%]	EN 196-3
počátek tuhnutí	188	[min]	EN 196-3
konec tuhnutí	257	[min]	EN 196-3
objemová stálost	1,0	[mm]	EN 196-3, Le Chatelier
měrný povrch	375	[m ² .kg ⁻¹]	EN 196-6, permeabilní metoda (Blaine)
střední zrno d(0,5)	20	[µm]	laserový granulometr
zbytek na síti	20 µm	39,8	[%] laserový granulometr
	45 µm	8,9	[%] laserový granulometr
	90 µm	0,2	[%] laserový granulometr
	125 µm	0,0	[%] laserový granulometr
	200 µm	0,0	[%] laserový granulometr
	250 µm	0,0	[%] laserový granulometr
měrná hmotnost	3110	[kg.m ⁻³]	ČSN EN 196-6
sypná hmotnost	v cisterně	980	[kg.m ⁻³] Přibližná hodnota při ložení cementu do autocisterny.
	v síle	1200-1600	[kg.m ⁻³] Odhad při uskladnění v síle. Sypná hmotnost se mění v závislosti na míře setřesení výrobku, době uskladnění nebo velikosti a zaplnění síla.
barevnost	L*	60	- Kolorimetrické měření v barevném prostoru CIELAB na cementu v práškové formě. Zdroj osvětlení D65 / 10°.
	a*	0	-
	b*	9	-
hydratační teplo	7 dní	300	[J.g ⁻¹] EN 196-8

Hodnoty uvedené v technickém listě mají čistě informativní charakter a mohou se lišit od hodnot konkrétních vzorků. Před jejich porovnáním s vlastnostmi jiných výrobků se prosím ujistěte, že všechna porovnávaná data byla získána pomocí totožných zkušebních postupů. V případě pochybností nás neváhejte kontaktovat.

CEM I 42,5 R

Portlandský cement

EN 197-1

Výrobní závod: **Mokrá**

Výrobce: **Českomoravský cement, a.s.**

Technický list

Vlastnost	Průměrná hodnota	Jednotka	Metoda / poznámka	
Chemické vlastnosti				
obsah	CaO	65	[%]	EN 196-2, XRF
	SiO ₂	19	[%]	EN 196-2, XRF
	Al ₂ O ₃	5	[%]	EN 196-2, XRF
	Fe ₂ O ₃	3	[%]	EN 196-2, XRF
	MgO	1	[%]	EN 196-2, XRF
	SO ₃	3,0	[%]	EN 196-2, XRF
	S ^{II-}	0,04	[%]	EN 196-2
	Cl ⁻	0,038	[%]	EN 196-2, XRF
	K ₂ O	0,82	[%]	EN 196-2, XRF
	Na ₂ O	0,12	[%]	EN 196-2, XRF
Na ₂ O ekvivalent		0,66	[%]	EN 196-2, XRF, (Na ₂ O + 0,658.K ₂ O)
nerozpustný zbytek		0,7	[%]	EN 196-2
ztráta žiháním		3,1	[%]	EN 196-2
Složení				
obsah slínku		90	[%]	Z hmotnosti konečného cementu, tj. včetně obsahu síranu vápenatého a případných přísad.
Složení slínku				
obsah	MgO	1,4	[%]	XRF
	C ₃ S	67	[%]	XRF, C ₃ S = 4,071.CaO - 1,4297.Fe ₂ O ₃ - 6,7187.Al ₂ O ₃ - 7,6024.SiO ₂
	C ₂ S	11	[%]	XRF, C ₂ S = - 3,071.CaO + 1,0785.Fe ₂ O ₃ + 5,0683.Al ₂ O ₃ + 8,6024.SiO ₂
	C ₃ A	7	[%]	XRF, C ₃ A = - 1,692.Fe ₂ O ₃ + 2,6504.Al ₂ O ₃
	C ₄ AF	11	[%]	XRF, C ₄ AF = 3,043.Fe ₂ O ₃

V případě, že je cement dodáván redukováný, obsahuje ve smyslu Nařízení Evropského parlamentu a Rady (ES) 1907/2006 přílohy XVII, čl. 47, redukční činidlo, které po smíchání s vodou snižuje obsah Cr6+ pod 0,0002 % a je účinné nejméně po dobu skladování cementu, po kterou musí být cement chráněn před působením vody a vysoké relativní vlhkosti vzduchu (nejvýše 75 %). Za těchto podmínek je redukční činidlo účinné 90 dnů od data uvedeného na obalu (balený cement) nebo od data expedice (volně ložený cement).

Hodnoty uvedené v technickém listě mají čistě informativní charakter a mohou se lišit od hodnot konkrétních vzorků. Před jejich porovnáním s vlastnostmi jiných výrobků se prosím ujistěte, že všechna porovnávaná data byla získána pomocí totožných zkušebních postupů. V případě pochybností nás neváhejte kontaktovat.

STACHEMENT 2180

Superplastifikační přísada



Skladování

V uzavřených plastových obalech je skladovatelnost 1 rok. Skladovat v teplotním rozmezí +5 až + 30°C. Chránit před silným zahřáním a před mrazem. Skladování pod 0°C může způsobit snížení účinnosti přísady, zmrznutí způsobuje trvalé znehodnocení. Výrobek je nehořlavý. Při skladování dodržujte platné právní předpisy BOZP a ochrany ŽP. Výrobek je vhodné pravidelně homogenizovat.

Balení a dodávání

- volně ložený v cisterně
- v návratných a zálohovaných 1000 litrových kontejnerech
- v nevratných 200 litrových PE sudech
- v nevratných malých PE obalech po 20, 50 litrech

Bezpečnost práce a ochrana zdraví

(podrobněji viz Bezpečnostní list výrobku)

Výrobek patří mezi mírně nebezpečné látky pro zdraví. Přítomné složky přísady mají mírně dráždivý účinek na pokožku a sliznici. Nebezpečné je požití přísady. Při práci s přísadou je třeba používat osobní ochranné pracovní pomůcky zabraňující přímému styku pokožky a očí, zejména ochranné pracovní rukavice a obličejový štít nebo ochranné brýle. Při vzniku aerosolů nebo prachu používat respirátor. Při práci nejíst, nepít, nekouřit. Před každou přestávkou a po skončení práce je třeba ruce důkladně umýt vodou a mýdlem, ošetřit regeneračním krémem.

První pomoc

(podrobněji viz Bezpečnostní list výrobku)

- při inhalaci par nebo dýmu vzniklém při požáru vynést postiženého na čerstvý vzduch, zajistit dýchání a zajistit lékařské ošetření
- při vniknutí do očí tyto důkladně vymýt velkým množstvím tekoucí vody po dobu 10 min. a vyhledat lékaře
- potřísněnou pokožku umýt vodou a mýdlem a ošetřit regeneračním krémem, např. Indulonou, v případě přetrvávajícího podráždění vyhledat lékaře
- při požití vypláchnout ústa vodou, vypít 0,2 - 0,5 litru chladné vody a vyhledat lékaře. Zvracení nevyvolávat, při spontánním zvracení zajistit, aby nedošlo k zadušení zvratky.

Ve všech vážnějších případech léčbu postiženého konzultovat:

Klinika nemocí z povolání, Toxikologické informační středisko, Na Bojišti 1, 128 08 Praha 2, tel. 224 91 92 93.

Upozornění

Technický list má pouze informativní charakter. Používání výrobku vyžaduje odzkoušení podle platných technických norem např. ČSN EN 206-1 apod.

Pro další dokumenty jako Certifikát, Prohlášení o vlastnostech/shodě, Bezpečnostní list, Podmínky pro skladování přísad apod. se obraťte na výrobce popř. dodavatele tohoto produktu.

Výrobce přísady je STACHEMA CZ s.r.o., Hasičská 1, 280 02, Kolín-Zibohlav, IČ: 46353747.

STACHEMA CZ s.r.o. nepřebírá odpovědnost za případné škody způsobené neodborným používáním výrobku a neručí za kvalitu výrobku plněného do obalů odběratele.

Datum revize: 22. 1. 2013

CE ISO 9001

C Matlab graphical output of image processing



Fig. 35: Color transformation of the UP-sample



Fig. 36: Color transformation of the U-sample



Fig. 37: Color transformation of the M-sample



Fig. 38: Color transformation of the IM-sample

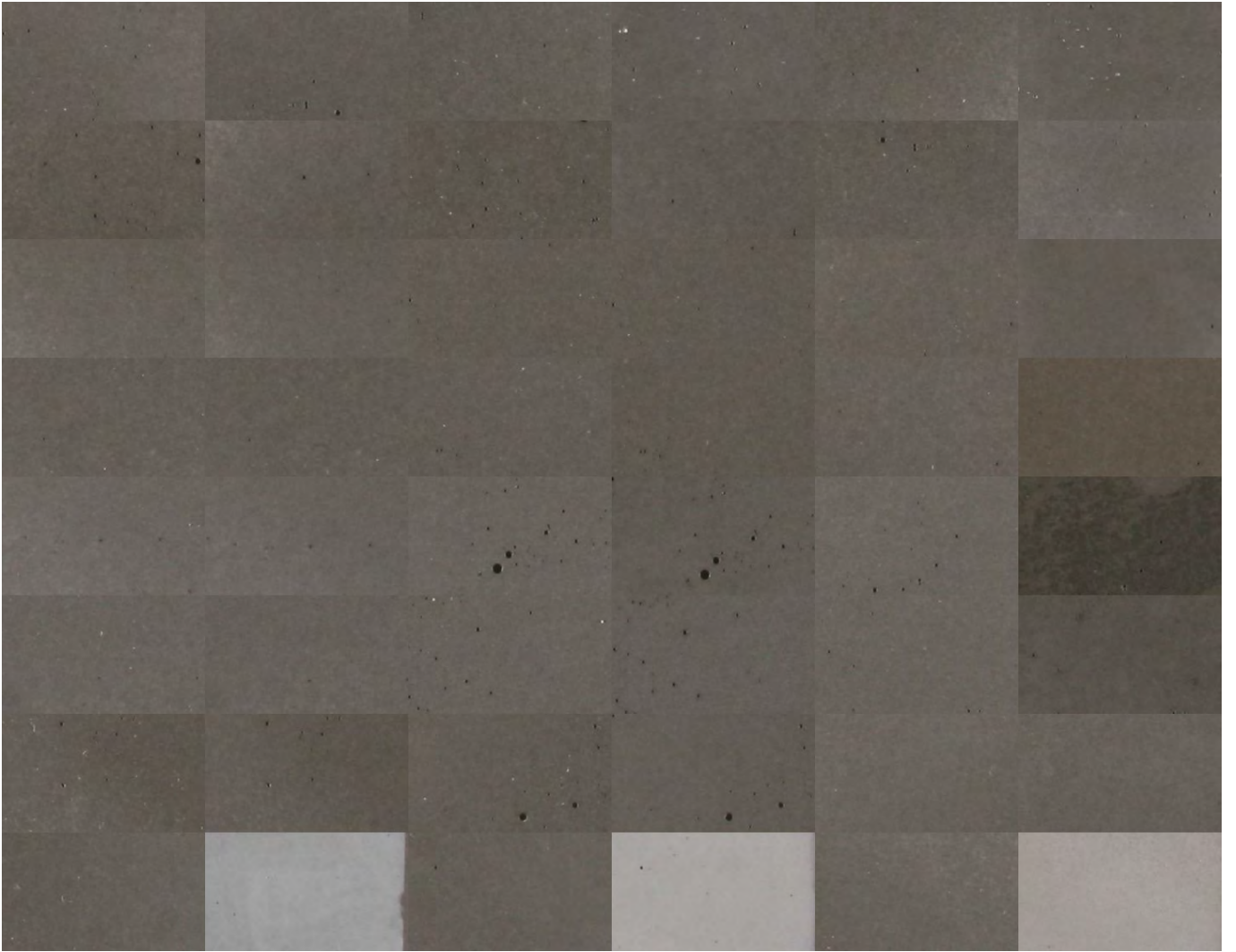


Fig. 39: Color transformation of the M+IM-sample